

A SELF-CONSISTENT-FIELD ITERATION FOR ORTHOGONAL CANONICAL CORRELATION ANALYSIS

LEIHONG ZHANG, LI WANG, ZHAOJUN BAI, AND REN-CANG LI

ABSTRACT. We propose an efficient algorithm for solving orthogonal canonical correlation analysis (OCCA) in the form of trace-fractional structure and orthogonal linear projections. Even though orthogonality has been widely used and proved to be a useful criterion for pattern recognition and feature extraction, existing methods for solving OCCA problem are either numerical unstable by relying on a deflation scheme, or less efficient by directly using generic optimization methods. In this paper, we propose an alternating numerical scheme whose core is the sub-maximization problem in the trace-fractional form with an orthogonal constraint. A customized self-consistent-field (SCF) iteration for this sub-maximization problem is devised. It is proved that the SCF iteration is globally convergent to a KKT point and that the alternating numerical scheme always converges. We further formulate a new trace-fractional maximization problem for orthogonal multiset CCA (OMCCA) and then propose an efficient algorithm with an either Jacobi-style or Gauss-Seidel-style updating scheme based on the same SCF iteration. Extensive experiments are conducted to evaluate the proposed algorithms against existing methods including two real world applications: multi-label classification and multi-view feature extraction. Experimental results show that our methods not only perform competitively to or better than baselines but also are more efficient.

1. INTRODUCTION

Canonical Correlation analysis (CCA) [12, 20] is a standard statistical technique and widely-used feature extraction paradigm for two sets of multidimensional variables. It finds basis vectors for the two sets of variables such that the correlations between the projections of the variables onto these basis vectors are mutually maximized.

During the last decade, CCA has received a renewed interest in the machine learning community. Many CCA variants have been proposed. Kernel CCA [3, 18] and neural networks [5] were introduced for exploring the nonlinear correlations. To deal with the underdetermined settings, regularization was introduced into CCA. Sparse CCA [45] was further proposed to facilitate the interpretation of the results through sparsity-inducing norms. Bayesian CCA [23] provided an alternative for

Leihong Zhang is with School of Mathematical Sciences, Soochow University, Suzhou 215006, Jiangsu, China. Email: longzlh@163.com.

Li Wang is with Department of Mathematics and Department of Computer Science and Engineering, University of Texas at Arlington, Arlington, TX 76019-0408, USA. Email: li.wang@uta.edu.

Zhaojun Bai is with Department of Computer Science and Department of Mathematics, University of California, Davis, CA 95616, USA. Email: zbai@ucdavis.edu.

Ren-cang Li is with Department of Mathematics, University of Texas at Arlington, Arlington, TX 76019-0408, USA. Email: rcli@uta.edu.

CCA to handle samples of small sizes and with noises. Semi-paired CCA [49] is able to handle the case where some of the observations in either view are missing. Multiset CCA [22, 31] extended CCA to find projections for more than two views.

The applicability of CCA has been demonstrated in various fields [43]. In machine learning community, CCA has been used for unsupervised data analysis when multiple views are available [14, 17], data fusion of multiple modalities [37], and reducing sample complexity of prediction problems using unlabeled data [21]. CCA becomes one popular tool for supervised learning, in which one view is derived from the data and the other view is derived from the class labels, such as multi-label classification [35, 41, 55]. More details about variants of CCA and their applications can be found in the recent survey [43].

In this paper, we are mainly interested in another variant of CCA, in which projections are linear and constrained to be orthogonal. Orthogonality is a widely used and effective criterion for pattern recognition and feature extraction. Orthogonality has been successfully adopted by various learning models. Linear discriminant analysis (LDA) with an orthogonality constraint often leads to better performance than conventional LDA since the orthogonality constraint to some extent can remove noise [48]. Orthogonal neighborhood preserving projections [26] is proposed to achieve good representation of the global structure and be effective for data visualization. Orthogonal locality preserving indexing [9] shares the same locality preserving character as locality preserving indexing, but at the same time it requires the basis functions to be orthogonal so that the metric structure of the document space is preserved. Orthogonality has also been explored in CCA [12, 38]. In addition to the above-mentioned properties brought by the orthogonality such as less sensitive to noise, good for data visualization, and preserving metrics, OCCA specifically preserves the covariance of the original data, while CCA does not [12]. OCCA is also extended for more than two views [39].

Although OCCA brings additional advantages for data analysis, it no longer retains an analytic solution as CCA in terms of singular value decomposition (SVD). A common heuristic approach is to orthogonalize the basis vectors obtained by CCA. However, this produces a suboptimal solution for the OCCA problem. In [38], an incremental scheme is employed to produce current basis vectors with additional constraints to enforce the orthogonality with the previously computed basis vectors. We will point out in Section 2 that the incremental scheme relies on a numerically unstable generalized eigenvalue problem, so the set of basis vectors are not guaranteed to be mutually orthogonal. Often, the orthogonalization as a post-processing step is required to obtain a feasible solution. In [12], generic optimization methods for minimizing a smooth function over the product of the Stiefel manifolds are used to solve the OCCA problem. These methods usually converge to a local minimizer but they do not take the special trace-fractional structure of OCCA into consideration. As a result, they are usually less efficient than custom-made algorithms.

One of our goals of this paper is to design efficient algorithms for solving the OCCA problem with guaranteed theoretical convergence and numerical stabilizability. In order to fully explore the special trace-fractional structure of OCCA, we first uncover the connection of OCCA with an eigenvector-dependent nonlinear eigenvalue problem (NEP_v), and then naturally come up with a simple iterative method

whose numerical efficiency is guaranteed by a succinct but structure-exploiting self-consistent-field (SCF) iteration. Global convergence and local convergence of this customized algorithm are established.

Contributions. The main contributions of this paper are summarized as follows:

- We propose a novel algorithm OCCA-scf for solving OCCA in the form of a trace-fractional matrix optimization problem. The proposed algorithm is built upon an efficient and effective SCF iteration to solve a very special trace-ratio sub-maximization problem through taking the trace-fractional structure into account. It is proved that the SCF iteration is always convergent and, as a result, OCCA-scf is guaranteed to converge. It can also integrate the state-of-the-art eigensolvers within the iteration framework. Moreover, it guarantees the orthogonality of the computed basis vectors.
- We present a new OMCCA model with integrated weights for each pair of views and trace-fractional objective for correlations between any two views. By leveraging the same customized SCF iteration, a novel range constrained OMCCA algorithm is proposed with an either Jacobi-style or Gauss-Seidel-style updating scheme.
- Extensive experiments are conducted for evaluating the proposed algorithms against existing methods in terms of various measurements, including sensitivity analysis, correlation analysis, computation analysis, and data visualization. We further apply our methods for two real world applications: multi-label classification and multi-view feature extraction. Experimental results show that our methods not only perform competitively to or better than baselines but also are more efficient.

Paper organization. We first review several related CCA models and their orthogonal variants in Section 2. In Section 3, we propose a novel algorithm for solving OCCA problem. A customized SCF iteration is presented to solve the sub-maximization problem of the algorithm in Section 4. In Section 5, we develop a new algorithm for OMCCA by leveraging the same SCF iteration. Extensive experiments are conducted in Section 6. Finally, we conclude this work in Section 7.

Notation. $\mathbb{R}^{m \times n}$ is the set of $m \times n$ real matrices and $\mathbb{R}^n = \mathbb{R}^{n \times 1}$. $I_n \in \mathbb{R}^{n \times n}$ is the identity matrix, and $\mathbf{1}_n \in \mathbb{R}^n$ is the vector of all ones. $\|\mathbf{x}\|_2$ is the 2-norm of vector $\mathbf{x} \in \mathbb{R}^n$. For $B \in \mathbb{R}^{m \times n}$, $\mathcal{R}(B)$ is the column subspace and its singular values are denoted by $\sigma_i(B)$ for $i = 1, \dots, \min(m, n)$ arranged in the nonincreasing order. The thin SVD of B is the one $B = U\Sigma V^T$ such that $\Sigma \succ 0$ and $\|B\|_{\text{tr}} = \sum_{i=1}^{\text{rank}(B)} \sigma_i(B)$ is its trace norm (also known as the nuclear norm). When $m = n$, $\text{sym}(B) = (B + B^T)/2$; if B is also symmetric, then $\text{eig}(B) = \{\lambda_i(B)\}_{i=1}^n$ denotes the set of its eigenvalues (counted by multiplicities) arranged in the nonincreasing order, and $B \succ 0$ ($\succeq 0$) means that B is also positive definite (semi-definite). The Stiefel manifold [2]

$$\mathbb{O}^{n \times k} = \{X \in \mathbb{R}^{n \times k} : X^T X = I_k\},$$

is an embedded submanifold of $\mathbb{R}^{n \times k}$ endowed with the standard inner product $\langle X, Y \rangle = \text{tr}(X^T Y)$ for $X, Y \in \mathbb{R}^{n \times k}$, where $\text{tr}(X^T Y)$ is the trace of $X^T Y$. Moreover, the tangent space $\mathcal{T}_X \mathbb{O}^{n \times k}$ of $\mathbb{O}^{n \times k}$ at $X \in \mathbb{O}^{n \times k}$ is given by (see e.g., [2])

$$(1) \quad \mathcal{T}_X \mathbb{O}^{n \times k} = \left\{ H \in \mathbb{R}^{n \times k} \left| \begin{array}{l} H = XK + (I_n - XX^T)J \\ \forall K = -K^T \in \mathbb{R}^{k \times k}, J \in \mathbb{R}^{n \times k} \end{array} \right. \right\}.$$

2. RELATED WORK

We review some representatives of CCA methods and their extension to multiple sets of variables.

2.1. Canonical Correlation Analysis. Canonical Correlation Analysis (CCA) is a two-view multivariate statistical method [20], where the variables of observations can be partitioned into two sets, i.e., the two views of the data. Denote the data matrices $S_1 \in \mathbb{R}^{n \times q}$ and $S_2 \in \mathbb{R}^{m \times q}$ from view 1 and view 2 with n and m features, respectively, where q is the number of samples. Assume both S_1 and S_2 are centralized, i.e., $S_1 \mathbf{1}_q = 0$ and $S_2 \mathbf{1}_q = 0$; otherwise, we may preprocess S_i as $S_i \leftarrow S_i - \frac{1}{q}(S_i \mathbf{1}_q) \mathbf{1}_q^T$, $i = 1, 2$. Let $\mathbf{x}_1 \in \mathbb{R}^n$ and $\mathbf{x}_2 \in \mathbb{R}^m$ be the canonical weight vectors. The canonical variates are the linear transformations defined as $\mathbf{z}_1 = S_1^T \mathbf{x}_1$, $\mathbf{z}_2 = S_2^T \mathbf{x}_2$. The canonical correlation between the two canonical variates is defined as $\rho(\mathbf{x}_1, \mathbf{x}_2) = \frac{\mathbf{z}_1^T \mathbf{z}_2}{\|\mathbf{z}_1\|_2 \|\mathbf{z}_2\|_2}$. CCA aims to find the pair of canonical weight vectors that maximize the canonical correlation:

$$(2) \quad \max_{\mathbf{x}_1, \mathbf{x}_2} \rho(\mathbf{x}_1, \mathbf{x}_2).$$

It can also be interpreted as the problem of finding the best pair of canonical weight vectors so that the cosine of the angle between two canonical variates is maximized, that is, the smallest angle in $[0, \frac{\pi}{2}]$.

This single-vector CCA (2) has been extended to obtain the pair of canonical weight matrices, namely, the pair of canonical weight matrices $X_1 \in \mathbb{R}^{n \times k}$ and $X_2 \in \mathbb{R}^{m \times k}$ by solving the following optimization problem

$$(3) \quad \max_{X_1, X_2} \text{tr}(X_1^T C_{1,2} X_2), \text{ s.t. } X_i^T C_{i,i} X_i = I_k, i = 1, 2,$$

where $C_{i,j} = S_i S_j^T$, $i, j = 1, 2$. In general, the closed-form solution of (3) can be obtained by SVD, and indeed, it can be proved that there is an optimal solution (X_1, X_2) so that $X_1^T C_{1,2} X_2 \succeq 0$ [11, Theorem III.2].

Traditional CCA is not suitable for settings where an orthogonal projection is required such as for data visualization in an orthogonal coordinate system. This is because optimal X_1 and X_2 in (3) usually do not have orthonormal columns. One can orthogonalize the columns of the optimal X_1 and X_2 to the problem (3) as a post-processing step, but it is generally suboptimal. For that reason, orthogonal CCA (OCCA) [12] is proposed to maximize the correlation

$$f(X, Y) = \frac{\text{tr}(X_1^T C_{1,2} X_2)}{\sqrt{\text{tr}(X_1^T C_{1,1} X_1) \text{tr}(X_2^T C_{2,2} X_2)}}$$

directly over orthonormal matrices, i.e.,

$$(4) \quad \max_{X_1 \in \mathbb{O}^{n \times k}, X_2 \in \mathbb{O}^{m \times k}} f(X, Y).$$

As pointed in [12], OCCA is different from traditional CCA because OCCA preserves the covariance of the original data S_1 and S_2 by finding orthonormal matrices where correlation is maximized, while traditional CCA whitens each dataset and orthogonally projects them so that the correlation is maximized. Generic optimization methods for minimizing/maximizing a smooth function over the product of the

Stiefel manifolds are available; for example, classical optimization algorithms such as the steepest descent gradient or the trust-region methods over the Euclidean space have been extended to the general Riemannian manifolds in, for example, [2]; however, besides only guaranteeing to converge to a local optimizer at best, these generic algorithms do not make use of the special trace-fractional structure in (4), and therefore, they usually are less efficient than custom-made algorithms for trace-ratio-related optimizations (see [52, 53] for some numerical results of trace-ratio optimizations).

The motivation of imposing orthogonality constraints was also explored in [38]. A greedy method (which we will call OCCA-SSY for short) is employed to find k pairs of orthogonal vectors, computed one pair at a time. The initial step is the same as traditional CCA to find the pair of canonical weight vectors $(\mathbf{x}_1^{(1)}, \mathbf{x}_2^{(1)})$ that solves (2). Given $\{(\mathbf{x}_1^{(t)}, \mathbf{x}_2^{(t)})\}_{t=1}^r$, the $(r + 1)$ st step is to solve the following problem

$$\begin{aligned} (\mathbf{x}_1^{(r+1)}, \mathbf{x}_2^{(r+1)}) &= \arg \max_{\mathbf{x}_1, \mathbf{x}_2} \rho(\mathbf{x}_1, \mathbf{x}_2) \\ \text{s.t. } \mathbf{x}_j^T C_{j,j} \mathbf{x}_j &= 1, \mathbf{x}_j^T \mathbf{x}_j^{(t)} = 0, j = 1, 2, t = 1, \dots, r. \end{aligned}$$

Such an approach relies on a deflation scheme, and the pair $(\mathbf{x}_1^{(r+1)}, \mathbf{x}_2^{(r+1)})$ is claimed to correspond to the dominant eigenpair of a generalized eigenvalue problem, which, however, numerically may not have any real eigenpair and thus is numerically unusable¹.

2.2. Multiset Canonical Correlation Analysis. Multiset CCA (MCCA) [22, 31] is proposed to analyze linear relationships among more than two canonical variates. It is a generalization of traditional CCA [20]. Here, we briefly introduce one widely used model [31] by seeking projections to maximize the sum of the pairwise correlation between any two canonical variates. Specifically, given ℓ datasets in the form of matrices

$$(5) \quad S_i \in \mathbb{R}^{n_i \times q} \quad \text{for } i = 1, 2, \dots, \ell,$$

where n_i is the number of features in the i th dataset, and q is the number of data points in each of the datasets. Without loss of generality, we may assume that all S_i are centered, i.e., $S_i \mathbf{1}_q = 0$ for all i .

Let $C_{i,j} = S_i S_j^T$ for $i, j = 1, \dots, \ell$. MCCA seeks to find the set of ℓ canonical weight vectors that solve

$$\max_{\mathbf{x}_1, \dots, \mathbf{x}_\ell} \sum_{i,j=1}^{\ell} \mathbf{x}_i^T C_{i,j} \mathbf{x}_j$$

subject to

$$(6) \quad \text{either } \sum_{i=1}^{\ell} \mathbf{x}_i^T C_{i,i} \mathbf{x}_i = 1,$$

$$(7) \quad \text{or } \mathbf{x}_i^T C_{i,i} \mathbf{x}_i = 1, i = 1, \dots, \ell.$$

¹Private communications with the authors of [38], 2019.

KKT conditions for MCCA under either (6) or (7) can be found in [31]. In particular, under (6), the condition is a generalized eigenvalue problem [31, p.297], which can be solved by any mature eigensolver [7, 16].

In [39], a greedy OMCCA (which we will call OMCCA-SS for short) was proposed, similarly to [38]. Recursively, it goes as follows. Given $\{\mathbf{x}_i^{(t)}, \forall i = 1, \dots, \ell, t = 1, \dots, r\}$, OMCCA-SS solves the following problem

$$\begin{aligned} \{\mathbf{x}_1^{(r+1)}, \dots, \mathbf{x}_\ell^{(r+1)}\} &= \arg \max_{\mathbf{x}_1, \dots, \mathbf{x}_\ell} \sum_{i,j=1}^{\ell} \mathbf{x}_i^T C_{i,j} \mathbf{x}_j, \\ \text{s.t. (6) and } \mathbf{x}_i^T \mathbf{x}_i^{(t)} &= 0, i = 1, \dots, \ell, t = 1, \dots, r. \end{aligned}$$

This OMCCA-SS method inherits the same issues as OCCA-SSY discussed in Subsection 2.1.

3. NOVEL ALGORITHM FOR ORTHOGONAL CCA

In this section we propose a new optimization scheme for solving (4), taking advantage of its special form.

3.1. Problem Formulation. Following the settings of all CCA methods, both views of the data S_1 and S_2 are centralized in advance. Define

$$A = S_1 S_1^T \in \mathbb{R}^{n \times n}, \quad B = S_2 S_2^T \in \mathbb{R}^{m \times m}, \quad C = S_1 S_2^T \in \mathbb{R}^{n \times m},$$

and, let $X \in \mathbb{O}^{n \times k}$ and $Y \in \mathbb{O}^{m \times k}$ have orthonormal columns. Given an integer $1 \leq k < \min\{m, n\}$ (usually $k \ll \min\{m, n\}$), we consider, instead of tackling problem (4) directly,

$$(8) \quad \max_{X \in \mathbb{O}^{n \times k}, Y \in \mathbb{O}^{m \times k}} \left\{ F(X, Y) := \frac{\text{tr}^2(X^T C Y)}{\text{tr}(X^T A X) \text{tr}(Y^T B Y)} \right\}.$$

Evidently, (4) and (8) are equivalent. In the next subsection we will develop a new algorithm based on (8). Our algorithm can take the advantage of the specific structure of the problem with theoretical guarantees, and more importantly, can be extended easily to handle the OMCCA model in Section 5.

3.2. The Proposed Algorithm. We propose the numerical scheme as shown in Algorithm 1. Although the framework of the proposed numerical scheme is rather natural, i.e., maximizing $F(X, Y)$ (or equivalently $f(X, Y)$) alternatively with respect to X and Y , the real novelty lies in the way how its core sub-maximization problems (9) and (10) are solved, which is the subject of Section 4 later.

The role of line 4 in Algorithm 1 is to make sure $X^{(\nu)}$ and $Y^{(\nu)}$ are always well aligned. It is particularly important when $X^{(\nu)}$ and $Y^{(\nu)}$ are approximations that are not best possibly accurate in the working precision. Its motivation is based on the structure of the function $F(X, Y)$: Given a pair $(X^{(\nu)}, Y^{(\nu)})$, the denominator is unchanged when this pair is changed to $(X^{(\nu)}U, Y^{(\nu)}V)$ for any $U, V \in \mathbb{O}^{k \times k}$, while the numerator is maximized by the particular pair $(U, V) = (\tilde{U}, \tilde{V})$ given by (see e.g., [13, 16])

$$(\tilde{U}, \tilde{V}) = \arg \max_{U, V \in \mathbb{O}^{k \times k}} \text{tr} \left(U^T (X^{(\nu)})^T C Y^{(\nu)} V \right),$$

whose solution, according to the following technical Lemma 1, can be achieved by, e.g., the SVD at line 4 of Algorithm 1, and the maximum is $\sum_{i=1}^k \sigma_i ((X^{(\nu)})^T C Y^{(\nu)})$.

Algorithm 1 An alternative optimization scheme for (8)

Input: $\{X^{(0)}, Y^{(0)}\}$ with $X^{(0)} \in \mathbb{O}^{n \times k}, Y^{(0)} \in \mathbb{O}^{m \times k}$.

Output: a solution $\{X^{(\nu)}, Y^{(\nu)}\}$ to (8).

- 1: **for** $\nu = 1, 2, \dots$ until convergence **do**
- 2: Solve

$$(9) \quad X^{(\nu)} \in \arg \max_{X \in \mathbb{O}^{n \times k}} F(X, Y^{(\nu-1)}).$$

- 3: Solve

$$(10) \quad Y^{(\nu)} \in \arg \max_{Y \in \mathbb{O}^{m \times k}} F(X^{(\nu)}, Y).$$

- 4: Compute SVD of $(X^{(\nu)})^T C Y^{(\nu)} = \tilde{U} \tilde{\Sigma} \tilde{V}^T$ and set $X^{(\nu)} \leftarrow X^{(\nu)} \tilde{U}$ and $Y^{(\nu)} \leftarrow Y^{(\nu)} \tilde{V}$;

- 5: **end for**

- 6: **return** $\{X^{(\nu)}, Y^{(\nu)}\}$ as a numerical solution to (8).
-

Lemma 1. *Let $W \in \mathbb{R}^{k \times k}$. Then $|\text{tr}(W)| \leq \sum_{i=1}^k \sigma_i(W)$. If, however, $|\text{tr}(W)| = \sum_{i=1}^k \sigma_i(W)$, then W is symmetric and is either positive or negative semidefinite.*

We also notice by Lemma 1, that such additional refinement step brings another nice property for the sequence $\{X^{(\nu)}, Y^{(\nu)}\}$, that is, $(X^{(\nu)})^T C Y^{(\nu)}$ is symmetric and positive semidefinite, which is a necessary condition for any global solution $\{X_{\text{opt}}, Y_{\text{opt}}\}$ (see Theorem 1(i)). Moreover, by using the effective solvers for (9) and (10), Algorithm 1 always converges. We summarize these results in the following theorem:

Theorem 1. *Let $\{X_{\text{opt}}, Y_{\text{opt}}\}$ be the optimal solution to (8) and $\{X^{(\nu)}, Y^{(\nu)}\}$ be the ν th approximation of Algorithm 1. Then*

- (i) $X_{\text{opt}}^T C Y_{\text{opt}}$ is symmetric and positive/negative semidefinite.
- (ii) $(X^{(\nu)})^T C Y^{(\nu)}$ is symmetric and positive semidefinite for $\nu \geq 1$, and thus for any limit pair $\{X, Y\}$ of $\{X^{(\nu)}, Y^{(\nu)}\}_{\nu=1}^{\infty}$, $X^T C Y$ is symmetric and positive semidefinite.
- (iii) The sequence $\{F(X^{(\nu)}, Y^{(\nu)})\}_{\nu=1}^{\infty}$ is monotonically increasing and converges.

The efficiency of Algorithm 1 relies heavily on solving the sub-maximization problems (9) and (10). Abstractly, they are of the following type

$$(11) \quad \max_{G \in \mathbb{O}^{n \times k}} \eta(G) \quad \text{with } \eta(G) := \frac{\text{tr}^2(G^T D)}{\text{tr}(G^T A G)},$$

where $0 \neq D \in \mathbb{R}^{n \times k}$ and $A \succ 0$. In Section 4, we present an SCF iteration that directly aims at solving (11).

4. AN SCF ITERATION FOR (11)

It can be seen that the global maximum of (11) is positive unless $D = 0$. Moreover, (11) is very much like the trace ratio (or trace quotient) maximization, i.e., maximizing $\text{tr}(G^T A_1 G) / \text{tr}(G^T A_2 G)$ over $G \in \mathbb{O}^{n \times k}$ with given $A_1, A_2 \succ 0$, for which an efficient SCF iteration is available [51, 29, 50]. It has been proved that the SCF iteration is globally convergent and the convergence is locally quadratic. We would like to mention that the SCF iteration was commonly used to solve the Eigenvector-Dependent Nonlinear Eigenvalue Problem (NEPv) [10] from the Kohn–Sham density functional theory in electronic structure calculations [30, 36]. Lately, it has been attracting a great deal attention in data science (e.g., [6, 10, 44, 52, 53]).

4.1. A nonlinear eigenvalue problem. We will first derive the formula for the partial derivative $\partial\eta(G)/\partial G$, where all entries G are treated as independent variables, and then the formula for the gradient $\text{grad}\eta(G)$ at $G \in \mathbb{O}^{n \times k}$ on the Stiefel manifold $\mathbb{O}^{n \times k}$ is given by (see e.g., [2])

$$(12) \quad \text{grad}\eta(G) = \Pi_G \left(\frac{\partial\eta(G)}{\partial G} \right) \in \mathcal{T}_G \mathbb{O}^{n \times k},$$

where $\Pi_G(Z) = Z - G \text{sym}(G^T Z)$ for $Z \in \mathbb{R}^{n \times k}$. By calculations, we have

$$\frac{\partial\eta(G)}{\partial G} = \frac{2\phi_D}{\phi_A} D - \frac{2\phi_D^2}{\phi_A^2} AG,$$

where, for convenience, we let $\phi_D \equiv \phi_D(G) = \text{tr}(G^T D)$ and $\phi_A \equiv \phi_A(G) = \text{tr}(G^T AG)$. Finally, use (12) to get

$$-\frac{\xi^2(G)}{2} \text{grad}\eta(G) = [AG - \xi(G)D] - GM(G) \in \mathbb{R}^{n \times k},$$

where

$$(13) \quad \xi(G) = \frac{\phi_A}{\phi_D}, \quad M(G) = \text{sym}(G^T AG - \xi(G)G^T D) \in \mathbb{R}^{k \times k}.$$

The discussion so far partially proved the KKT condition for (11) in Lemma 2.

Lemma 2. *If G is a maximizer of (11), then $G^T D = D^T G$ and*

$$(14) \quad AG - \xi(G)D = GM(G).$$

Note that the condition (14) is a type of nonlinear Sylvester equation but with the orthogonality constraint $G^T G = I_k$. To solve it, we will convert it into an NEPv so that certain type of SCF is applicable. One straightforward way is to use the constraint $G^T G = I_k$ and then rewrite (14) equivalently as $[A - \xi(G)DG^T]G = GM(G)$. However, we notice that the matrix $A - \xi(G)DG^T$ is not necessarily symmetric, even at a maximizer G . This means that we cannot ensure $A - \xi(G)DG^T$ has real eigenvalues at $G \in \mathbb{O}^{n \times k}$. To overcome that obstacle, we construct the following NEPv instead:

$$(15) \quad E(G)G = G\widehat{M}(G),$$

where $\widehat{M}(G) = G^T E(G)G \in \mathbb{R}^{k \times k}$ and

$$E(G) := A - \xi(G)(DG^T + GD^T).$$

Evidently, $E(G)$ is always symmetric. The following lemma establishes a relation between (15) and (14).

Lemma 3. *Suppose $G \in \mathbb{O}^{n \times k}$. Then G satisfies (14) if and only if G is an eigenbasis matrix of $E(G)$, i.e., G satisfies (15).*

This lemma characterizes any maximizer G of (11) as an orthonormal eigenbasis matrix of $E(G)$. By (15), we find

$$\text{eig}(\widehat{M}(G)) = \{\lambda_{\pi_1}(E(G)), \dots, \lambda_{\pi_k}(E(G))\} \subseteq \text{eig}(E(G)),$$

where $\{\pi_1 \leq \dots \leq \pi_k\} \subset \{1, 2, \dots, n\}$. A followup question is where the eigenvalues $\lambda_{\pi_i}(E(G))$ are located within $\text{eig}(E(G))$. In the next two subsections, we will investigate this issue and the investigation yields important necessary conditions for local and global maximizers of (11).

4.2. Eigenspace associated with a local maximizer. Even though our maximization problem (11) is very much like the trace ratio problem [51], unfortunately, it does not enjoy some nice properties as the trace ratio problem (for example, it is shown that any local maximizer of the trace ratio problem is also a global solution). In Example 1 below, we will see numerically that (11) may admit local but non-global maximizers.

Example 1. Consider the case with $n = 5$, $k = 2$,

$$A = \begin{bmatrix} 4 & 0 & -5 & -5 & 1 \\ 0 & 2 & 1 & -1 & 1 \\ -5 & 1 & 9 & 5 & 1 \\ -5 & -1 & 5 & 18 & 4 \\ -1 & 1 & 1 & 4 & 2 \end{bmatrix} \quad \text{and} \quad D = \begin{bmatrix} -1 & 1 \\ 0 & 0 \\ 0 & 2 \\ 0 & 0 \\ 1 & 0 \end{bmatrix}.$$

By calling the MATLAB function `fmincon`, we find two (numerical) local maximizers:

$$G_+ = \begin{bmatrix} -0.358041496119094 & 0.770164268103322 \\ -0.453284095949462 & -0.326431512218038 \\ -0.091335437376569 & 0.497561512998402 \\ -0.269574025133855 & 0.008593213179154 \\ 0.765066989399257 & 0.229451880441015 \end{bmatrix},$$

$$G_* = \begin{bmatrix} -0.506648923972689 & 0.664385053189626 \\ 0.619602876311725 & 0.312889763321350 \\ -0.337893503149209 & 0.384494340924914 \\ 0.103073503143856 & 0.210902556071053 \\ -0.484358314662567 & -0.518050876600301 \end{bmatrix}.$$

It is computed that $\eta(G_+) \approx 2.303 < \eta(G_*) \approx 10.16$. We argue that they are local maximizers. First the norms of the corresponding gradients at G_+ and G_* are less than 10^{-6} . Second, by sampling randomly 10^7 tangent vectors H in the form of (1), we found that for both G_+ and G_* , the following second order sufficient condition to be given in (16) hold, implying that both are local maximizers. This example numerically shows (11) in general admits local but non-global maximizers.

The following lemma presents second-order necessary and sufficient conditions for local maximizers [32, 47].

Lemma 4. *Let G be a local maximizer of (11). Then for all nonzero $H \in \mathbb{R}^{n \times k}$ satisfying $H^T G = -G^T H$, it holds that*

$$(16) \quad \text{tr}^2(D^T H) \leq \eta(G) \left(\text{tr}(H^T A H) - \text{tr}(H M(G) H^T) \right),$$

where $M(G)$ is given in (13). Conversely, if the inequality (16) is strict, then G is a local maximizer.

Corollary 1. *If G is a local maximizer of (11), then we have*

$$(17) \quad \text{tr}(K^T (G^T A G - M(G)) K) \geq 0, \forall K = -K^T \in \mathbb{R}^{k \times k},$$

and moreover, for all $J \in \mathbb{R}^{n \times k}$,

$$\begin{aligned}
(18) \quad & \frac{\left(\operatorname{tr}(D^T J) - \operatorname{tr}(G^T D J^T G)\right)^2}{\eta(G)} \leq \operatorname{tr}(J^T E(G) J) \\
& - \operatorname{tr}(J^T G M(G) G^T J) + \xi(G) \operatorname{tr}(J^T G D^T G G^T J) \\
& + \operatorname{tr}(G^T J M(G) J^T G) - \operatorname{tr}(J M(G) J^T),
\end{aligned}$$

where $\xi(G)$ is given in (13).

Theorem 2. *Suppose G is a local maximizer of (11). Then $\mathcal{R}(G)$ is an eigenspace of $E(G)$ associated with eigenvalues $\lambda_{\pi_1}(E(G)) \leq \dots \leq \lambda_{\pi_k}(E(G))$ satisfying $\pi_1 \leq k$.*

Theorem 2 indicates that for any local maximizer G , the smallest eigenvalue associated with the eigenspace $\mathcal{R}(G)$ must be smaller than $\lambda_k(E(G))$. This offers a necessary condition for a KKT point to be a local maximizer. As a much stronger version, we will show in the next subsection that any global maximizer G must be an eigenbasis matrix associated with the k smallest eigenvalues of $E(G)$.

4.3. Eigenspace associated with a global maximizer. The results in Lemma 5 and Theorem 3 hold keys to characterize the global maximizer and to establish an SCF iteration for (11).

Lemma 5. *For any $G, \widehat{G} \in \mathbb{O}^{n \times k}$, if $\widehat{G}^T D = D^T \widehat{G} \succeq 0$ and*

$$(19) \quad \operatorname{tr}(\widehat{G}^T E(G) \widehat{G}) \leq \operatorname{tr}(G^T E(G) G),$$

then $\eta(\widehat{G}) \geq \eta(G)$. Furthermore, if the inequality in (19) is strict, then $\eta(\widehat{G}) > \eta(G)$.

Theorem 3. *Suppose G_{opt} is a global maximizer to (11). Then G_{opt} is an orthonormal eigenbasis matrix associated with the k smallest eigenvalues of $E(G_{\text{opt}})$. Moreover, the matrix $G_{\text{opt}}^T D$ is symmetric and either positive or negative semidefinite.*

Returning to Example 1 with the computed G_+ and G_* , we observe that both G_+ and G_* are (approximately) the orthonormal eigenbasis matrix of $E(G_+)$ and $E(G_*)$, respectively.

4.4. A self-consistent-field (SCF) iteration. Equipped with the necessary condition in Theorem 3, we propose an SCF iteration as outlined in Algorithm 2 to solve NEPv (15) for the purpose of solving (11).

Algorithm 2 An SCF iteration for solving (11)

Input: $G_{(0)} \in \mathbb{O}^{n \times k}$;

Output: approximate maximizer G to (11).

- 1: **for** $\nu = 1, 2, \dots$ until convergence **do**
 - 2: construct $E_{(\nu)} = E(G_{(\nu-1)})$ as in (15);
 - 3: compute an orthonormal eigenbasis matrix $G_{(\nu)}$ associated with the k smallest eigenvalues of $E_{(\nu)}$;
 - 4: compute the SVD of $G_{(\nu)}^T D = U \Sigma V^T$ and update $G_{(\nu)} \leftarrow G_{(\nu)} U V^T$;
 - 5: **end for**
 - 6: **return** the last $G_{(\nu)}$ as a numerical maximizer of (11).
-

Remark 1. Line 3 in Algorithm 2 is justified by Lemma 5 because the chosen $G_{(\nu)}$ satisfies

$$\mathrm{tr}(G_{(\nu)}^T E(G_{(\nu-1)}) G_{(\nu)}) \leq \mathrm{tr}(G_{(\nu-1)}^T E(G_{(\nu-1)}) G_{(\nu-1)})$$

and thus $\eta(G_{(\nu)}) \geq \eta(G_{(\nu-1)})$. To understand line 4, we note that an eigenbasis matrix is not unique. In fact, $\widehat{G}_{(\nu)} = G_{(\nu)} P$ for any $P \in \mathbb{O}^{k \times k}$ is also one. Since $\mathrm{tr}(\widehat{G}_{(\nu)}^T A \widehat{G}_{(\nu)}) \equiv \mathrm{tr}(G_{(\nu)}^T A G_{(\nu)})$ but $\mathrm{tr}^2(\widehat{G}_{(\nu)}^T D) \neq \mathrm{tr}^2(G_{(\nu)}^T D)$ in general, it makes sense to update $G_{(\nu)}$ to $\widehat{G}_{(\nu)}$ so that $\mathrm{tr}^2(\widehat{G}_{(\nu)}^T D)$ is maximized over $P \in \mathbb{O}^{k \times k}$. That is when Lemma 1 comes to help.

Because an eigenbasis matrix is not unique, one may ask if $G_{(\nu)}$ at line 4 in Algorithm 2 is well-defined. The next theorem addresses this issue.

Theorem 4. *At line 3 of Algorithm 2, if the eigenvalue gap*

$$\zeta_{\nu-1} = \lambda_{k+1}(E(G_{(\nu-1)})) - \lambda_k(E(G_{(\nu-1)})) > 0,$$

then any two orthonormal eigenbasis matrices $\widehat{G}_{(\nu)}$ and $\widetilde{G}_{(\nu)}$ associated with k smallest eigenvalues of $E(G_{(\nu-1)})$ satisfy $\widetilde{G}_{(\nu)} = \widehat{G}_{(\nu)} Q$ for some orthogonal matrix $Q \in \mathbb{O}^{k \times k}$. Furthermore, if additionally $\mathrm{rank}(D^T \widehat{G}_{(\nu)}) = k$, then the next approximation $G_{(\nu)}$ from line 4 of Algorithm 2 is uniquely determined.

4.5. Convergence analysis. We next provide some basic convergence properties of the simple SCF iteration (Algorithm 2) for solving (11).

Theorem 5. *Let the sequence $\{G_{(\nu)}\}$ be generated by the SCF iteration (Algorithm 2). Then*

- (i) *For each $\nu \geq 1$, $D^T G_{(\nu)} \succeq 0$ and $\mathrm{tr}(G_{(\nu)}^T D) = \sum_{j=1}^k \sigma_j(G_{(\nu)}^T D)$;*
- (ii) *The sequence $\{\eta(G_{(\nu)})\}$ is monotonically increasing and convergent;*
- (iii) *If*

$$(20) \quad \begin{aligned} & \mathrm{tr}(G_{(\nu)}^T E(G_{(\nu-1)}) G_{(\nu)}) \\ & < \mathrm{tr}(G_{(\nu-1)}^T E(G_{(\nu-1)}) G_{(\nu-1)}), \end{aligned}$$

then $\eta(G_{(\nu-1)}) < \eta(G_{(\nu)})$;

- (iv) *$\{G_{(\nu)}\}$ has a convergent subsequence $\{G_{(\nu)}\}_{\nu \in \mathcal{I}}$;*
- (v) *Let $\{G_{(\nu)}\}_{\nu \in \mathcal{I}}$ be any convergent subsequence of $\{G_{(\nu)}\}$ with the accumulation point G_* satisfying*

$$(21) \quad \zeta = \lambda_{k+1}(E(G_*)) - \lambda_k(E(G_*)) > 0.$$

Then G_ satisfies the first order optimality condition in Lemma 2 and also the necessary condition for a global minimizer in Theorem 3.*

Remark 2. We have three remarks for Theorem 5.

- (a) Item (iii) of Theorem 5 implies that, to only guarantee monotonicity of $\{\eta(G_{(\nu)})\}$, the partial eigen-decomposition in line 3 of Algorithm 2 can be inexact. In particular, in line 3, we can choose any approximation $G_{(\nu)} \in \mathbb{O}^{n \times k}$ satisfying (20), and then refine it by line 4 to ensure $D^T G_{(\nu)} \succeq 0$; by Lemma 5, $\eta(G_{(\nu)}) > \eta(G_{(\nu-1)})$ holds too. This facilitates us to employ certain sophisticated eigensolver for the computation task in line 3.
- (b) Item (iv) is rather obvious because $\{G_{(\nu)}\}$ is a bounded sequence in $\mathbb{R}^{n \times k}$. It is explicitly listed to substantiate part of the assumption in item (v). A stronger claim in Theorem 6 later says the entire sequence $\{G_{(\nu)}\}$ converges under a mild condition.

- (c) Item (v) shows one of advantages of our SCF iteration over the generic Riemannian optimization methods for solving the core subproblem (11). In particular, as our SCF iteration is built upon the necessary conditions of the global maximizer G_{opt} , besides the general KKT conditions, the convergent point also fulfills certain necessary conditions for being a global maximizer.

For further analyzing convergence of the sequence $\{G_{(\nu)}\}$, we now consider the sequence $\{\mathcal{R}(G_{(\nu)})\}$ of subspaces. For this purpose, we denote by $\|\cdot\|_{\text{ui}}$ any unitarily invariant norm, and introduce the distance measure between two subspaces \mathcal{G} and \mathcal{Y} of dimension k [40, p.95]

$$(22) \quad \text{dist}_{\text{ui}}(\mathcal{G}, \mathcal{Y}) := \|\sin \Theta(\mathcal{G}, \mathcal{Y})\|_{\text{ui}}$$

in terms of the matrix of canonical angles between \mathcal{G} and \mathcal{Y} :

$$\Theta(\mathcal{G}, \mathcal{Y}) = \text{Diag}(\theta_1(\mathcal{G}, \mathcal{Y}), \dots, \theta_k(\mathcal{G}, \mathcal{Y})).$$

Let $\mathcal{G} = \mathcal{R}(G)$ and $\mathcal{Y} = \mathcal{R}(Y)$, where $G, Y \in \mathbb{R}^{n \times k}$ with $G^T G = Y^T Y = I_k$. The canonical angles $\theta_1(\mathcal{G}, \mathcal{Y}) \geq \dots \geq \theta_k(\mathcal{G}, \mathcal{Y})$ is defined by

$$0 \leq \theta_i(\mathcal{G}, \mathcal{Y}) := \arccos \sigma_i(G^T Y) \leq \frac{\pi}{2} \quad \text{for } 1 \leq i \leq k.$$

The collection of all k -dimensional subspaces in \mathbb{R}^n is the so-called Grassmann manifold $\mathcal{G}_k(\mathbb{R}^n)$, and (22) is a unitarily invariant metric [40, p.95] on $\mathcal{G}_k(\mathbb{R}^n)$. For the trace norm, also known as the nuclear norm, we have

$$\text{dist}_{\text{tr}}(\mathcal{G}, \mathcal{Y}) = \sum_{j=1}^k \sin \theta_j(\mathcal{G}, \mathcal{Y}).$$

Using the metric $\text{dist}_{\text{tr}}(\mathcal{G}, \mathcal{Y})$, we have the following convergence result for the sequence $\{G_{(\nu)}\}$ by the SCF iteration in Algorithm 2.

Theorem 6. *Let the sequence $\{G_{(\nu)}\}$ be generated by the SCF iteration (Algorithm 2), and let G_* be an accumulation point of $\{G_{(\nu)}\}$.*

- (i) *If $\mathcal{R}(G_*)$ is an isolated accumulation point (in the metric (22)) of $\{\mathcal{R}(G_{(\nu)})\}_{\nu=0}^{\infty}$, then $\{\mathcal{R}(G_{(\nu)})\}_{\nu=0}^{\infty}$ converges to $\mathcal{R}(G_*)$.*
- (ii) *If also $\text{rank}(G_*^T D) = k$, then $\{G_{(\nu)}\}_{\nu=0}^{\infty}$ converges to G_* (in the standard Euclidean metric), and for sufficiently large ν ,*

$$(23) \quad \text{dist}_{\text{tr}}(\mathcal{R}(G_*), \mathcal{R}(G_{(\nu+1)})) \leq c_0 \|G_{(\nu)} - G_*\|_{\text{tr}},$$

where

$$c_0 = \frac{3\|D\|_2}{\zeta} \left(\sqrt{\frac{\|A\|_{(k)}}{\eta(G_*)}} + 2k \frac{\|A\|_2 + \sqrt{\frac{\|A\|_{(k)}}{\eta(G_*)}} \|D\|_2}{\sqrt{\eta(G_*) \omega_k(A)}} \right),$$

with $\|A\|_{(k)} = \sum_{j=1}^k \sigma_j(A)$, $\omega_k(A) = \sum_{j=1}^k \sigma_{n-j+1}(A)$, and the eigenvalue gap $\zeta > 0$ is given in (21).

5. ORTHOGONAL MULTISSET CCA

In this section, we propose to solve a new formulation of OMCCA based on the proposed methods in Sections 3 and 4.

5.1. Problem Formulation. Let S_i and $C_{i,j}$ be the ones defined in Subsection 2.2. Related to notion of the set of canonical weight matrices for MCCA, similarly to (3), a general model is to seek canonical weight matrices $X_i \in \mathbb{R}^{n_i \times k}$ that solve

$$(24) \quad \max_{\{X_i\}} f(\{X_i\}), \quad \text{s.t. } X_i^T C_{i,i} X_i = I_k, \quad i = 1, \dots, \ell,$$

where $1 \leq k \leq \min\{n_1, \dots, n_\ell, q\}$, and

$$(25) \quad f(\{X_i\}) = \sum_{\substack{i,j=1 \\ i \neq j}}^{\ell} \rho_{ij} \frac{\text{tr}(X_i^T C_{i,j} X_j)}{\sqrt{\text{tr}(X_i^T C_{i,i} X_i)} \sqrt{\text{tr}(X_j^T C_{j,j} X_j)}},$$

with some weighting factors $\rho_{ij} \geq 0$ which will not only dictate the contribution of the correlation between S_i and S_j to the total $f(\{X_i\})$ but also, as we will see later, dramatically reduce the number terms in $f(\{X_i\})$ and thus speed up computations. Most of all, we assume that judiciously chosen ρ_{ij} with only a few of them nonzero can in fact improve the performances of multi-view tasks, which will be verified by the experiments. Analogously to (4), OMCCA naturally arises:

$$(26) \quad \max_{\{X_i \in \mathbb{O}^{n_i \times k}\}} f(\{X_i\}).$$

Ideally, the optimal weights should be learned from data, but this is out of the scope for this paper. Hence, we take some heuristic weighting schemes. To begin with, we define

$$(27) \quad \hat{\rho}_{ij} = \frac{\sum_{r=1}^{\text{rank}(C_{i,j})} \sigma_r(C_{i,j})}{\sqrt{\text{tr}(C_{i,i}) \text{tr}(C_{j,j})}}, \quad \text{for } i, j = 1, \dots, \ell.$$

It is known $0 \leq \hat{\rho}_{ij} \leq 1$ [19, (3.5.22) on p.212]. Envision a graph of ℓ nodes corresponding to dataset X_i , respectively, with every two nodes connected with an edge whose weight is to be determined. We now explain our heuristic strategies to select the weights.

- (1) uniform weighting: $\hat{\rho}_{ij} = 1, \forall i, j = 1, \dots, \ell$.
- (2) tree weighting: find the minimal spanning tree of the graph with the edge (i, j) having weight $1 - \hat{\rho}_{ij}$, record the spanning tree with its edge weights reset back to $\hat{\rho}_{ij}$ and weights $\hat{\rho}_{ij}$ for all other edges not in the tree reset to 0.
- (3) top- p weighting: find the p largest weights among $\hat{\rho}_{ij}$ for $i > j$, and reset all other weights $\hat{\rho}_{ij}$ to 0.

Next we apply the soft-max function over those selected weights $\hat{\rho}_{ij}$ with a bandwidth parameter (e.g., 20 used in our experiments) to yield ρ_{ij} to use in (25). As a by-product, the sum of all ρ_{ij} is 1.

Unfortunately, there does not seem to have an efficient way to solve (24) or (26), beyond primitive optimization techniques such as plain gradient ascent iteration or the trust-region methods. Next, we extend Algorithm 1 for $\ell = 2$ to solve (26).

5.2. The Proposed Algorithm. Problem (26) cannot be simply solved by maximizing each individual term in $f(\{X_i\})$ of (25) separately; otherwise each dataset would have more than one projection matrix X_i . What we plan to do, based on the machinery we have built in the previous sections, is to optimize $f(\{X_i\})$ cyclically over each matrix variable X_i in the styles similar to either the Jacobi or Gauss-Seidel iteration for linear systems [13]. Specifically, we establish an inner-outer iterative method to solve (26). The most outer iteration – each step called a cycle –

generates from the current approximation $\{X_i^{(\nu)}\}_{i=1}^\ell$ to the next $\{X_i^{(\nu+1)}\}_{i=1}^\ell$ of the maximizer of (26); each cycle can be of an either Jacobi-style or Gauss-Seidel-style updating scheme that relies on the proposed novel SCF iteration for solving a series of subproblems in the form of (11).

Due to the possibility that $\text{rank}(C_{i,i}) \leq \min\{n_i - 1, q\}$ and possibly $q \ll n_i$, numerical difficulties may arise and will arise when $q \ll n_i$. To circumvent them, we propose to add range constraints

$$(28) \quad \mathcal{R}(X_i) \subset \mathcal{R}(S_i) \quad \text{for } i = 1, 2, \dots, \ell.$$

In what follows, we describe an SVD-based implementation. Let the SVDs of S_i be

$$(29) \quad S_i = U_i \Sigma_i V_i^T, \quad U_i \in \mathbb{R}^{n_i \times r_i}, \quad V_i \in \mathbb{R}^{q \times r_i}, \quad \Sigma_i \in \mathbb{R}^{r_i \times r_i},$$

where $r_i = \text{rank}(S_i)$. With the SVDs in (29), we have

$$X_i^T S_i S_j^T X_j = X_i^T U_i \Sigma_i V_i^T V_j \Sigma_j U_j^T X_j =: \widehat{X}_i^T \Sigma_i V_i^T V_j \Sigma_j \widehat{X}_j,$$

where $\widehat{X}_i = U_i^T X_i \in \mathbb{R}^{r_i \times k}$. Under (28), we will have $X_i = U_i \widehat{X}_i$. The function $f(\{X_i\})$ is then transformed into

$$\sum_{i \neq j} \rho_{ij} \frac{\text{tr}(\widehat{X}_i^T \Sigma_i V_i^T V_j \Sigma_j \widehat{X}_j)}{\sqrt{\text{tr}(\widehat{X}_i^T \Sigma_i^2 \widehat{X}_i)} \sqrt{\text{tr}(\widehat{X}_j^T \Sigma_j^2 \widehat{X}_j)}} =: g(\{\widehat{X}_i\}),$$

and

$$\max_{X_i \in \mathbb{O}^{n_i \times k}, \mathcal{R}(X_i) \subset \mathcal{R}(S_i), \forall i} f(\{X_i\}) = \max_{\widehat{X}_i \in \mathbb{O}^{r_i \times k}, \forall i} g(\{\widehat{X}_i\}).$$

The key step to maximize $g(\{\widehat{X}_i\})$ by either the Jacobi- or Gauss-Seidel-style updating scheme is to maximize it, for any $s \in \{1, \dots, \ell\}$, over \widehat{X}_s while keeping all other \widehat{X}_j for $j \neq s$. That is equivalent to

$$(30) \quad \max_{\widehat{X}_s \in \mathbb{O}^{n_s \times k}} \frac{\text{tr}(\widehat{X}_s^T D_s)}{\sqrt{\text{tr}(\widehat{X}_s^T \Sigma_s^2 \widehat{X}_s)}},$$

where

$$(31) \quad D_s(\{\widehat{X}_i\}_{i \neq s}) = \Sigma_s V_s^T \sum_{j \neq s} \rho_{sj} \frac{V_j \Sigma_j \widehat{X}_j}{\sqrt{\text{tr}(\widehat{X}_j^T \Sigma_j^2 \widehat{X}_j)}}.$$

Problem (30) is equivalent to solving:

$$(32) \quad \max_{\widehat{X}_s \in \mathbb{O}^{n_s \times k}} \frac{\text{tr}^2(\widehat{X}_s^T D_s)}{\text{tr}(\widehat{X}_s^T \Sigma_s^2 \widehat{X}_s)},$$

which takes the same form as (11), the subject of which has been studied in Section 4.

Algorithm 3 outlines the framework of two inner-outer numerical methods, where each cycle (lines 6–9) follows either the Jacobi-style or Gauss-Seidel-style updating scheme. A couple of comments are in order for efficiently implementing Algorithm 3.

First, evaluating all D_s as written in (31) is rather costly when majority or all of ρ_{ij} are nonzero. But in the case when all ρ_{ij} are the same, say 1, there are many common terms among all D_s for $s = 1, 2, \dots, \ell$, and that should be taken advantage of. However, for two weighting strategies – tree weighting and top- p weighting, we previously discussed, most D_s only has very few terms in its summation and evaluating D_s is not a concern at all.

Algorithm 3 RCOMCCA: Range Constrained OMCCA

Input: $\{S_i \in \mathbb{R}^{n_i \times q}\}$ (each S_i is centered), integer $1 \leq k \leq \min\{\text{rank}(S_1), \dots, \text{rank}(S_\ell), q\}$, and a tolerance ϵ ;

Output: $\{X_i \in \mathbb{O}^{n_i \times k}\}$ that maximizes $f(\{X_i\})$.

- 1: compute the SVDs in (29);
- 2: pick an initial approximation $\widehat{X}_1^{(0)}$;
- 3: $\nu = 0, g = 0$;
- 4: **repeat**
- 5: $g_0 = g; g = 0$;
- 6: **for** $s = 1$ to ℓ **do**
- 7: compute the next $\{\widehat{X}_s^{(\nu+1)}\}$ by solving (32), where either
- (33) $D_s = D_s(\{\widehat{X}_i^{(\nu)}\}_{i \neq s})$
- for the Jacobi-style updating scheme, or
- (34) $D_s = D_s(\widehat{X}_1^{(\nu+1)}, \dots, \widehat{X}_{s-1}^{(\nu+1)}, \widehat{X}_{s+1}^{(\nu)}, \dots, \widehat{X}_\ell^{(\nu)})$
- for Gauss-Seidel-style updating scheme.
- 8: $g = g + g_s$, where g_s is the computed optimal objective value of (32).
- 9: **end for**
- 10: $\nu = \nu + 1$;
- 11: **until** $|g - g_0| \leq \epsilon g$;
- 12: **return** $X_i = U_i \widehat{X}_i^{(\nu)}$ for $1 \leq i \leq \ell$.

The second comment is that, for the Jacobi-style updating scheme, each sub-problem (32) is independent within one full cycle: line 6-9, and thus they can be solved in parallel. As in the case for the linear system [13], often the Gauss-Seidel-style updating scheme converges faster than the Jacobi-style updating scheme in terms of the cycle counts. However, sometimes, the built-in parallelism in the later may well compensate that disadvantage in the wall-clock.

6. EXPERIMENTS

6.1. Implementation details. For a practical implementation of the SCF in Algorithm 2, when the matrix size $n \leq 500$, we call the mex version `mexeig` of the LAPACK [4] eigen-decomposition subroutine `dsyevd`² to compute $G_{(\nu)}$, while for matrix size $n > 500$, we choose the locally optimal block preconditioned conjugate gradient method³ (`lobpcg`) (see [24, 25]) with the diagonal preconditioner $P = \text{Diag}(A)$ to compute an approximation orthonormal eigenbasis matrix $G_{(\nu)}$ in line 3. As `lobpcg` searches an approximation eigenbasis matrix $G_{(\nu)}$ by optimizing the Rayleigh quotient in a subspace containing $G_{(\nu-1)}$, the condition (20) is always fulfilled, meaning (by Theorem 5) that the sequence $\{\eta(G_{(\nu)})\}$ is monotonically increasing and convergent. The SCF iteration of Algorithm 2 terminates if $\nu > 30$ or

$$\frac{\|\text{grad}(\eta(G_{(\nu)}))\|_1}{\xi^2(G_{(\nu)})(\|A\|_1 + \|D\|_1)} \leq \epsilon_{\text{scf}} \text{ or } \left| \frac{\eta(G_{(\nu)}) - \eta(G_{(\nu-1)})}{\eta(G_{(\nu)})} \right| \leq \epsilon_{\text{scf}}^{3/2}$$

with $\epsilon_{\text{scf}} = 10^{-5}$ and $\xi(G_{(\nu)})$ is defined in (13).

²`mexeig` (available at: www.math.nus.edu.sg/~matsundf/) is a MATLAB interface to call LAPACK eigen-decomposition subroutine `dsyevd` of a real symmetric matrix.

³The MATLAB version of `lobpcg` is available at: <http://cn.mathworks.com/matlabcentral/fileexchange/48-lobpcg-m>.

6.2. Comparisons with generic optimization methods. We conduct extensive experiments to compare our SCF-based alternative iteration (Algorithm 1) with three generic optimization methods over matrix manifolds implemented in LDR toolbox⁴ [12]. They are `stiefel`, `stiefel_trust`, and `stiefel_trust_prod` for solving problem (4) (i.e., $\ell = 2$). In particular, `stiefel`, `stiefel_trust` are based similarly on our scheme in Algorithm 1 to update X and Y alternatively, but solve the subproblems (11) by the generic Riemannian steepest gradient iteration and the Riemannian trust-region method [2], respectively; the third one `stiefel_trust_prod` just employs the plain Riemannian Trust-Region (RTR) of [2] to solve (4) directly. We use the default settings of these three algorithms coded in the LDR toolbox, in which `stiefel`, `stiefel_trust` stop whenever the number of alternative steps $\nu > 100$ or

$$(35) \quad \left| \frac{f(X^{(\nu)}, Y^{(\nu)}) - f(X^{(\nu-1)}, Y^{(\nu-1)})}{f(X^{(\nu)}, Y^{(\nu)})} \right| \leq \epsilon_{\text{alt}},$$

with $\epsilon_{\text{alt}} = 10^{-8}$, whereas `stiefel_trust_prod` uses the default setting of RTR [1] in the package `manopt`. For comparisons, we terminate our SCF-based Algorithm 1 if $\nu > 30$ or when the norm of Riemannian gradient $\text{grad_norm} = \|\text{grad}F(X^{(\nu)}, Y^{(\nu)})\|_2 \leq \epsilon_{\text{alt}}$ or (35) holds with $F(X, Y)$ instead of $f(X, Y)$.

Our experiments are performed over a synthetic data with $m = n = 1000$ by varying $k \in [3, 100]$, and the yeast data shown in Table 1 with $m = 101, n = 14$ by varying $k \in [2, 14]$. Following in [12], we generate the synthetic data with $q = 10^4$ and two views controlled by two sets of latent variables W and Z as follows:

$$\begin{aligned} d_z &= \left\lceil \frac{\max(m, n)}{2} \right\rceil, d_w = \left\lceil \frac{2 \max(m, n)}{5} \right\rceil, \\ S_X &= P_X Z + Q_X W + \lambda E_X, \\ S_Y &= P_Y Z + Q_Y W + \lambda E_Y, \end{aligned}$$

where $Z \in \mathbb{R}^{d_z \times q}$, $W \in \mathbb{R}^{d_w \times q}$, $P_X \in \mathbb{R}^{m \times d_z}$, $Q_X \in \mathbb{R}^{m \times d_w}$, $P_Y \in \mathbb{R}^{n \times d_z}$, $Q_Y \in \mathbb{R}^{n \times d_w}$, $E_X \in \mathbb{R}^{m \times q}$, and $E_Y \in \mathbb{R}^{n \times q}$ are matrices where each entry is i.i.d. sampled from a normal distribution with zero mean and unit standard deviation, and $\lambda = 2 \times 10^{-4}$.

The performance is evaluated in terms of the following criteria:

- (1) Computational complexity measured by CPU time;
- (2) The correlation difference. The differences of the objective values between the SCF-based iteration and each of the other three methods are reported. The larger the difference is, the better the SCF-based iteration performs than the other;
- (3) The gradient norm `grad_norm` at the computed solution.

Fig. 1 shows the numerical results obtained by four different methods (all starting with the initial guess $\{X^{(0)}, Y^{(0)}\} = \{I_{n,k}, I_{m,k}\}$ where $I_{n,k}$ contains the first k columns of I_n) in terms of three performance measurements over the synthetic data and yeast for multi-label classification. We have the following observations:

- (1) For small k , our SCF-based alternative iteration converges much faster than others. The time cost of SCF-based method is similar to `stiefel`, while `stiefel_trust` is most expensive among all.
- (2) The SCF-based iteration obtains the similar correlation values on both data with `stiefel_trust` and `stiefel_trust_prod`. `stiefel` is the worst, and also

⁴<https://github.com/cunni/ldr>

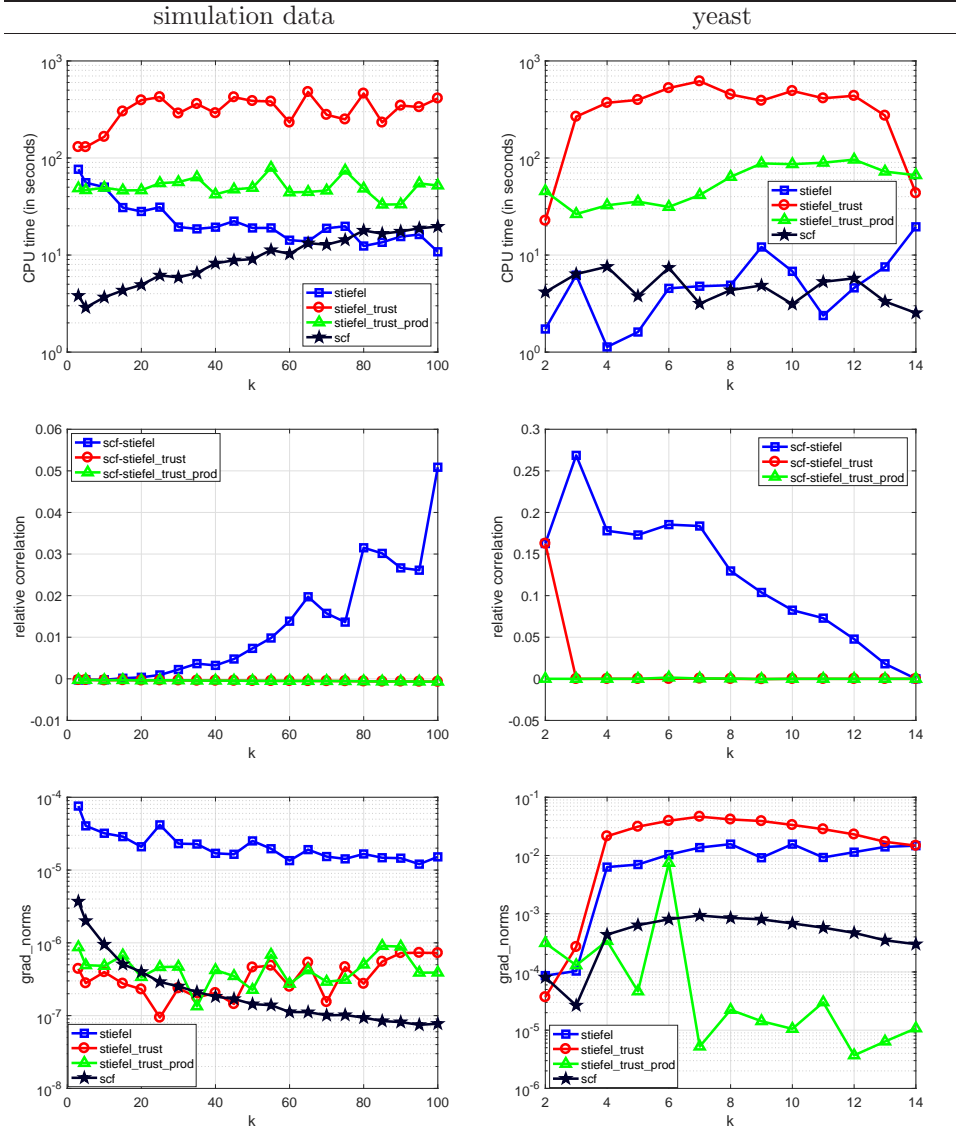


FIGURE 1. The comparison of four optimization methods in terms of three different criteria evaluated on the synthetic data and real multi-label classification data yeast.

the correlations over various k values demonstrate opposite trends on the synthetic data and yeast. This implies that stiefel is quite sensitive to the value k and the input data.

- (3) Overall, our SCF-based iteration is an efficient way to solve the two-view OCCA problem (4). Except for consuming more CPU time, stiefel_trust_prod is also able to compute an accurate approximation; however, our SCF-based iteration can be easily extended to solve the more general MOCCA model (26) in the framework of Algorithm 3, and thus naturally, we choose it as

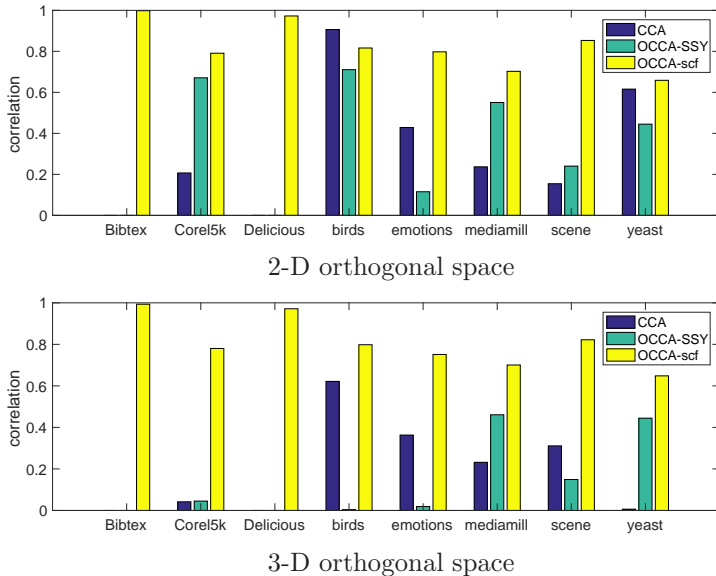


FIGURE 2. The correlations obtained by three CCA methods in the 2-D and 3-D orthogonal spaces.

a core engine for subproblems in line 7 of Algorithm 3 in our subsequent experiments.

6.3. Correlation Analysis and Data Visualization. In this section, we first explore the embedded subspaces obtained by three different CCA methods: classical CCA, OCCA-SSY and OCCA-scf. For data visualization, the orthogonal space in 2-D and 3-D are the main focus. As aforementioned, the classical CCA method does not generate the orthonormal basis matrices for projection, and OCCA-SSY method also does not guarantee to generate the orthonormal basis matrices either. To obtain orthonormal basis matrices, we post-orthogonalize the matrices obtained by CCA and OCCA-SSY. If the matrices is rank deficient, we set the correlation as zero since the number of orthogonal basis vectors is smaller than requested. Fig. 2 shows the comparisons of three CCA methods in terms of the correlation score over eight real data in Table 1 for multi-label classification problems (detailed description is presented in Section 6.4.1). It is obvious that our proposed OCCA-scf achieves the best performance among all. More importantly, our method never encounters the matrix rank deficient issue, while this happens for CCA and OCCA-SSY on some datasets, such as Bibtex and Delicious.

We then explore the embeddings in 2-D and 3-D spaces and examine the correlations between the input data and its multi-label outputs. Since each sample may have multiple labels, we transform the output labels into the multi-class classification problem using the label powerset approach [8] for the purpose of data visualization. The set of multiclass labels consists of all unique label combinations found in the data. For example, the data scene has 6 labels, and there are 15 unique label combinations in total. Fig. 3 shows the embeddings of both input and output in 2-D and 3-D spaces colored by unique classes. Since multiple data points are assigned to the same unique class, there are only 15 embedded output points. In

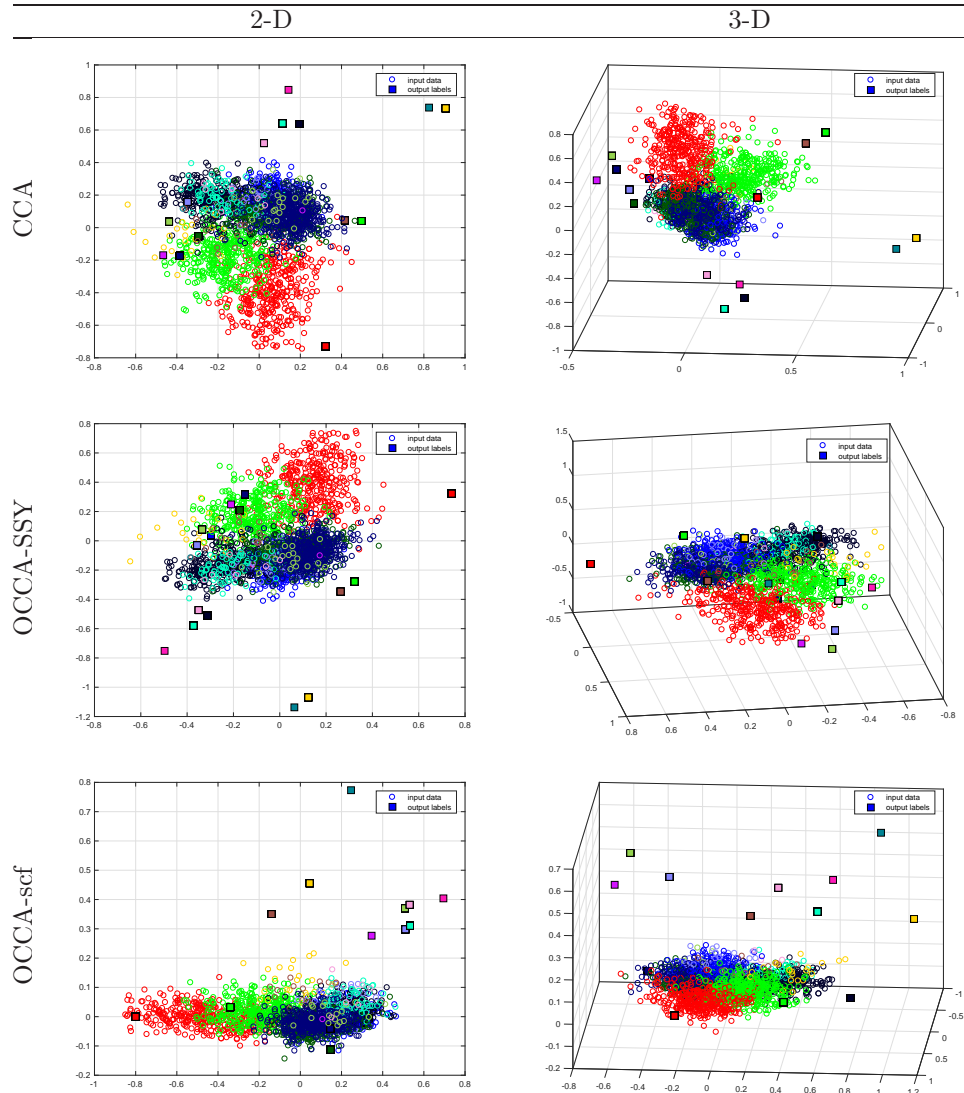


FIGURE 3. The comparisons of three OCCA methods in terms of 2-D and 3-D embeddings evaluated on scene data. Colors represents classes. The markers circle and square represent the input data points and the output classes. We show one class for each input data and output label although there are 15 classes extracted from 6 multiple labels.

the cases of both 2-D and 3-D, our OCCA-scf method show the best alignments between input data and output labels, for example, the majority of classes such as the red, green and blue ones show the better alignment in the reduced space with the input data clouds than other two methods. In addition to correlation analysis and data visualization, we will evaluate the multi-label classification problems in terms of various popularly used measurements in Section 6.4.1.

TABLE 1. Multi-label classification datasets

Dataset	Samples	Attributes	labels
birds	645	260	19
Corel5k	5000	499	374
emotions	593	72	6
scene	2407	294	6
yeast	2417	101	14
Bibtex	7395	1836	159
Mediamill	43903	120	101
Delicious	16105	500	983

6.4. Applications. We evaluate our proposed methods in terms of two real-world applications, multi-label classification and multi-view feature extraction, where various CCA methods have been explored in the literature [41, 39]. Since multi-label classification inherently corresponds to the two-view problem, we evaluate the proposed OCCA-scf method in Algorithm 1 against baselines. For multi-view feature extraction, the proposed RCOMCCA in Algorithm 3 is evaluated over more than two views.

6.4.1. Multi-label classification. Multi-label classification [42] is a variant of the classification problem, where one instance may have various number of labels from a set of predefined categories, i.e., a subset of labels. It is different from multi-class classification problem, where each instance only has a single label. In general, the output class labels of one instance are represented by the indicator vector of size m where m is the number of class labels. If the c th label is assigned to the instance, the c th element of the indicator vector is 1, and otherwise 0. Let $X \in \mathbb{R}^{n \times q}$ be the q instances of size n and $Y \in \mathbb{R}^{m \times q}$ be comprised of the q indicator vectors. The popular use of CCA for multi-label classification is to treat X to be one view and Y as the other view [41, 55, 35].

The multi-label classification datasets used in our experiments are shown in Table 1. All datasets are publicly available⁵. Following [41], we take CCA as a supervised dimensionality reduction step for multi-label classification so that the embeddings obtained by CCA methods can encode certain correlations among input data and labels. Hence, it expects to have better performance for multi-label classification. Since some datasets have a small number of output labels, the reduced dimension is up-bounded by the number of output labels due to the inherent property of CCA. To alleviate the limitation from CCA and improve the classification performance for general datasets, we propose to augment the learned embeddings using the original input data through a simple concatenation over two sets of features.

In this paper, we choose to use ML-kNN⁶ as our backend multi-label classifier [54], which has demonstrated good performance over various datasets. We compare our OCCA-scf with other CCA methods including OCCA-SSY [38], LS-CCA [41] and classical CCA. All CCA-based methods take ML-kNN as the base classifier and corresponding augmentation approach for each CCA method is indicated by the suffix “-aug”. We randomly split the data into 40% for training and 60% for testing and tune the neighborhood parameter within the set $\{1, 3, 5, 7, 9, 13, 15\}$ for

⁵<http://mulan.sourceforge.net/datasets-mlc.html>

⁶<http://lamda.nju.edu.cn/files/MLkNN.rar>

TABLE 2. Results on five datasets in terms of the 5 measurements(40% for training and 60% for testing over 10 random splits). Best results are in bold.

dataset	method	HammingLoss	RankingLoss	OneError	Coverage	Average_Precision
birds	OCCA-scf	0.0503 \pm 0.0035	0.2173 \pm 0.0062	0.4964 \pm 0.0201	2.8866 \pm 0.1580	0.5452 \pm 0.0118
	OCCA-scf-aug	0.0545 \pm 0.0026	0.3045 \pm 0.0047	0.7101 \pm 0.0136	3.8597 \pm 0.1754	0.3942 \pm 0.0107
	CCA	0.1167 \pm 0.0095	0.3509 \pm 0.0197	0.8110 \pm 0.0302	4.2028 \pm 0.2954	0.3087 \pm 0.0192
	CCA-aug	0.0545 \pm 0.0026	0.3046 \pm 0.0046	0.7101 \pm 0.0136	3.8602 \pm 0.1745	0.3942 \pm 0.0107
	LS-CCA	0.1167 \pm 0.0095	0.3509 \pm 0.0197	0.8110 \pm 0.0302	4.2028 \pm 0.2954	0.3084 \pm 0.0191
	LS-CCA-aug	0.0545 \pm 0.0026	0.3046 \pm 0.0046	0.7101 \pm 0.0136	3.8602 \pm 0.1745	0.3942 \pm 0.0107
	OCCA-SSY	0.0618 \pm 0.0049	0.2669 \pm 0.0150	0.5978 \pm 0.0269	3.4499 \pm 0.2146	0.4722 \pm 0.0182
	OCCA-SSY-aug	0.0545 \pm 0.0026	0.3046 \pm 0.0046	0.7101 \pm 0.0136	3.8607 \pm 0.1752	0.3942 \pm 0.0108
	ML-kNN	0.0545 \pm 0.0026	0.3046 \pm 0.0046	0.7101 \pm 0.0136	3.8607 \pm 0.1752	0.3942 \pm 0.0108
	emotions	OCCA-scf	0.2283 \pm 0.0064	0.2016 \pm 0.0091	0.3258 \pm 0.0201	1.9643 \pm 0.0456
OCCA-scf-aug		0.2716 \pm 0.0057	0.2799 \pm 0.0098	0.3989 \pm 0.0171	2.3862 \pm 0.0573	0.6959 \pm 0.0085
CCA		0.2395 \pm 0.0090	0.2204 \pm 0.0138	0.3497 \pm 0.0169	2.0736 \pm 0.0730	0.7443 \pm 0.0126
CCA-aug		0.2718 \pm 0.0059	0.2801 \pm 0.0094	0.3986 \pm 0.0168	2.3860 \pm 0.0595	0.6960 \pm 0.0082
LS-CCA		0.2346 \pm 0.0084	0.2088 \pm 0.0149	0.3385 \pm 0.0182	2.0096 \pm 0.0930	0.7553 \pm 0.0154
LS-CCA-aug		0.2719 \pm 0.0056	0.2795 \pm 0.0099	0.3983 \pm 0.0172	2.3848 \pm 0.0572	0.6964 \pm 0.0085
OCCA-SSY		0.2577 \pm 0.0141	0.2543 \pm 0.0198	0.3860 \pm 0.0274	2.2309 \pm 0.0916	0.7190 \pm 0.0172
OCCA-SSY-aug		0.2719 \pm 0.0057	0.2800 \pm 0.0095	0.3986 \pm 0.0170	2.3862 \pm 0.0589	0.6958 \pm 0.0084
ML-kNN		0.2720 \pm 0.0057	0.2798 \pm 0.0097	0.3983 \pm 0.0169	2.3862 \pm 0.0589	0.6960 \pm 0.0085
Scene		OCCA-scf	0.1214 \pm 0.0024	0.1375 \pm 0.0070	0.3329 \pm 0.0073	0.7772 \pm 0.0360
	OCCA-scf-aug	0.0941 \pm 0.0016	0.0817 \pm 0.0028	0.2428 \pm 0.0081	0.4981 \pm 0.0154	0.8557 \pm 0.0041
	CCA	0.1267 \pm 0.0032	0.1448 \pm 0.0068	0.3451 \pm 0.0087	0.8153 \pm 0.0369	0.7810 \pm 0.0065
	CCA-aug	0.0949 \pm 0.0020	0.0820 \pm 0.0035	0.2440 \pm 0.0080	0.4999 \pm 0.0194	0.8555 \pm 0.0044
	LS-CCA	0.1228 \pm 0.0028	0.1401 \pm 0.0059	0.3361 \pm 0.0085	0.7909 \pm 0.0326	0.7873 \pm 0.0058
	LS-CCA-aug	0.0948 \pm 0.0021	0.0821 \pm 0.0034	0.2440 \pm 0.0082	0.5003 \pm 0.0187	0.8553 \pm 0.0044
	OCCA-SSY	0.1183 \pm 0.0030	0.1302 \pm 0.0055	0.3226 \pm 0.0086	0.7405 \pm 0.0314	0.7979 \pm 0.0063
	OCCA-SSY-aug	0.0943 \pm 0.0020	0.0818 \pm 0.0025	0.2431 \pm 0.0090	0.4981 \pm 0.0137	0.8558 \pm 0.0042
	ML-kNN	0.0949 \pm 0.0020	0.0823 \pm 0.0033	0.2442 \pm 0.0085	0.5009 \pm 0.0188	0.8554 \pm 0.0042
	Corel5k	OCCA-scf	0.0094 \pm 0.0000	0.1365 \pm 0.0015	0.7252 \pm 0.0055	116.3179 \pm 1.2727
OCCA-scf-aug		0.0094 \pm 0.0000	0.1373 \pm 0.0016	0.7309 \pm 0.0067	116.9343 \pm 1.3411	0.2474 \pm 0.0031
CCA		0.0094 \pm 0.0000	0.1396 \pm 0.0012	0.7519 \pm 0.0079	117.9406 \pm 1.1541	0.2339 \pm 0.0035
CCA-aug		0.0094 \pm 0.0000	0.1381 \pm 0.0016	0.7327 \pm 0.0056	117.3671 \pm 1.2944	0.2436 \pm 0.0031
LS-CCA		0.0095 \pm 0.0000	0.1379 \pm 0.0015	0.7432 \pm 0.0082	116.8526 \pm 1.3332	0.2463 \pm 0.0027
LS-CCA-aug		0.0094 \pm 0.0000	0.1376 \pm 0.0015	0.7323 \pm 0.0082	117.1294 \pm 1.2682	0.2459 \pm 0.0039
OCCA-SSY		0.0094 \pm 0.0000	0.1365 \pm 0.0015	0.7263 \pm 0.0085	116.4133 \pm 1.3187	0.2522 \pm 0.0038
OCCA-SSY-aug		0.0094 \pm 0.0000	0.1371 \pm 0.0016	0.7304 \pm 0.0054	116.8367 \pm 1.2580	0.2481 \pm 0.0032
ML-kNN		0.0094 \pm 0.0000	0.1381 \pm 0.0019	0.7323 \pm 0.0062	117.5434 \pm 1.4205	0.2434 \pm 0.0035
yeast		OCCA-scf	0.2080 \pm 0.0021	0.1838 \pm 0.0039	0.2538 \pm 0.0066	6.5615 \pm 0.0736
	OCCA-scf-aug	0.1997 \pm 0.0033	0.1735 \pm 0.0034	0.2356 \pm 0.0075	6.3870 \pm 0.0859	0.7556 \pm 0.0041
	CCA	0.2108 \pm 0.0031	0.1894 \pm 0.0056	0.2539 \pm 0.0069	6.6438 \pm 0.0969	0.7364 \pm 0.0054
	CCA-aug	0.2011 \pm 0.0026	0.1762 \pm 0.0035	0.2398 \pm 0.0068	6.4152 \pm 0.0827	0.7512 \pm 0.0040
	LS-CCA	0.2077 \pm 0.0038	0.1855 \pm 0.0044	0.2518 \pm 0.0092	6.5928 \pm 0.1040	0.7436 \pm 0.0054
	LS-CCA-aug	0.2012 \pm 0.0028	0.1760 \pm 0.0036	0.2405 \pm 0.0060	6.4096 \pm 0.0864	0.7511 \pm 0.0038
	OCCA-SSY	0.2097 \pm 0.0035	0.1871 \pm 0.0052	0.2526 \pm 0.0058	6.6265 \pm 0.1023	0.7403 \pm 0.0055
	OCCA-SSY-aug	0.1997 \pm 0.0033	0.1740 \pm 0.0033	0.2356 \pm 0.0074	6.3907 \pm 0.0984	0.7554 \pm 0.0036
	ML-kNN	0.2017 \pm 0.0029	0.1759 \pm 0.0036	0.2397 \pm 0.0067	6.4075 \pm 0.0831	0.7512 \pm 0.0036

ML-kNN. Following [54], we report the best results and their standard deviations over 10 random train/test splits in terms of the following five measurements:

- HammingLoss: the average number of times an instance-label pair is misclassified.
- RankingLoss: the average fraction of label pairs that are reversely ordered for the instance.
- OneError: the average number of times the top-ranked label is not in the set of proper labels of the instance
- Coverage: on the average how far we need to go down the list of labels in order to cover all the proper labels of the instance.
- AveragePrecision: the average precision of labels ranked above a particular label in the same label set.

Except AveragePrecision, the first four measurements show good performances of multi-label classification if the measurement value is small.

Table 2 shows the results obtained by compared methods over 5 datasets in terms of the 5 measurements. We observed that our OCCA-scf and OCCA-scf-aug

show better results on almost all the five measurements except Average_Precision on Scene by OCCA-SSY-aug. For datasets scene and yeast, OCCA-scf-aug shows better results than OCCA-scf. This implies that our augmentation approach is effective when the features obtained by dimensionality reduction method such as CCA somehow lose the information that is also useful for multi-label classification although the correlations remain. It is worth noting that our methods outperform ML-kNN over all the experimented datasets. These observations imply that CCA with orthogonality constraints improves ML-kNN for multi-label classification and our proposed OCCA-scf methods outperform other CCA methods.

TABLE 3. Multi-view datasets

Dataset	Samples	Multiple views	classes
mfeat	2000	216;76;64;6;240;47	10
Caltech101-7	1474	254;512;1180;1008;64;1000	7
Caltech101-20	2386	254;512;1180;1008;64;1000	20
Scene15	4310	254;512;531;360;64;1000	15
yeast_ribosomal	1040	3735;4901;441	2

6.4.2. *Multi-view feature extraction.* Previous experiments focus on the problems with only two views. Here, we aim to explore our proposed RCOMCCA for multiset canonical correlation analysis in terms of multi-view feature extraction [39, 38]. Following [38], we employ the serial fusion strategy to concatenate embeddings from all views for classification based on 1-nearest neighbor classifier. Since LDR-based CCA and LS-CCA are not easy to be extended for learning with multiple views, we compare our proposed RCOMCCA with MCCA [22, 31] and OMCCA-SS [39]. It is worth noting that RCOMCCA allows two updating scheme and is capable of integrating various weighting scheme. Hence, we name the variants of RCOMCCA by augmenting “-G” for Gauss-Seidel-style and “-J” for the Jacobi-style, together with three weighting schemes shown in bracket. As a result, there are six variants of RCOMCCA in total. For the top- p weighting scheme, $p \in \{1, 3, 6\}$ is used, except that $p \in \{1, 3\}$ is used for yeast_ribosomal.

The datasets with relevant statistics used for multi-view feature extraction are shown in Table 3. For image datasets such as Caltech101⁷[28] and Scene15⁸ [27], we apply various feature descriptors to extract features of views including CENTRIST [46], GIST [34], LBP [33], histogram of oriented gradient (HOG), color histogram (CH), and SIFT-SPM [27]. Note that we drop CH for Scene15 due to the gray-level images. mfeat is handwritten numeral data⁹ [15] with 6 views including 76 Fourier coefficients of the character shapes, 216 profile correlations, 64 Karhunen-Love coefficients, 240 pixel averages in 2×3 windows, 47 Zernike moments, and 6 morphological features. The Berkeley genomic dataset yeast_ribosomal¹⁰ is used where three aspects of the protein are considered as the views including Pfam HMM, Hydrophobicity FFT and Gene expression for binary classification problem, e.g., ribosomal vs. non-ribosomal.

⁷http://www.vision.caltech.edu/Image_Datasets/Caltech101/

⁸https://figshare.com/articles/15-Scene_Image_Dataset/7007177

⁹<https://archive.ics.uci.edu/ml/datasets/Multiple+Features>

¹⁰<https://noble.gs.washington.edu/proj/sdp-svm/>

TABLE 4. Means and standard deviations of accuracy obtained by 1-nearest neighbor classifier on each view and embeddings obtained by three CCA methods over 10 random drawn from each dataset (30% training and 70% testing). Parameter k used by CCA methods to achieve the best accuracy is shown in the bracket. The symbol “-” for the non-existence of the view.

	mfeat	Caltech101-7	Caltech101-20	Scene15	yeast_ribosomal
view1	0.9513 \pm 0.0053	0.9259 \pm 0.0049	0.7659 \pm 0.0046	0.5766 \pm 0.0091	0.8553 \pm 0.0472
view2	0.7604 \pm 0.0104	0.9443 \pm 0.0051	0.8257 \pm 0.0064	0.5269 \pm 0.0070	0.8831 \pm 0.0072
view3	0.9293 \pm 0.0043	0.9415 \pm 0.0070	0.8226 \pm 0.0106	0.5528 \pm 0.0081	0.9856 \pm 0.0046
view4	0.6780 \pm 0.0064	0.9287 \pm 0.0105	0.7968 \pm 0.0118	0.4609 \pm 0.0079	-
view5	0.9630 \pm 0.0025	0.7759 \pm 0.0133	0.6042 \pm 0.0122	0.6946 \pm 0.0130	-
view6	0.7814 \pm 0.0077	0.9152 \pm 0.0059	0.7645 \pm 0.0128	-	-
MCCA	0.8679 \pm 0.0073 (6)	0.8865 \pm 0.0072 (15)	0.8620 \pm 0.0072 (40)	0.6851 \pm 0.0043 (35)	0.8155 \pm 0.0139 (3)
OMCCA-SS	0.8298 \pm 0.0089 (6)	0.9493 \pm 0.0024 (45)	0.8527 \pm 0.0057 (50)	0.7030 \pm 0.0081 (50)	0.8379 \pm 0.0110 (5)
RCOMCCA-G (uniform)	0.7634 \pm 0.0134 (5)	0.8880 \pm 0.0052 (50)	0.7150 \pm 0.0075 (45)	0.4866 \pm 0.0044 (50)	0.8639 \pm 0.0291 (40)
RCOMCCA-G (top- p)	0.9696 \pm 0.0035 (5)	0.9664 \pm 0.0060 (35)	0.8887 \pm 0.0077 (25)	0.7542 \pm 0.0054 (30)	0.8756 \pm 0.0095 (45)
RCOMCCA-G (tree)	0.9566 \pm 0.0031 (6)	0.9392 \pm 0.0043 (45)	0.7882 \pm 0.0078 (50)	0.4004 \pm 0.0063 (30)	0.8678 \pm 0.0161 (45)
RCOMCCA-J (uniform)	0.7540 \pm 0.0121 (5)	0.8868 \pm 0.0068 (30)	0.7350 \pm 0.0091 (50)	0.4995 \pm 0.0059 (50)	0.8492 \pm 0.0201 (35)
RCOMCCA-J (top- p)	0.9692 \pm 0.0038 (5)	0.9649 \pm 0.0029 (15)	0.8893 \pm 0.0074 (25)	0.7574 \pm 0.0077 (30)	0.8782 \pm 0.0071 (35)
RCOMCCA-J (tree)	0.9581 \pm 0.0055 (6)	0.9474 \pm 0.0041 (45)	0.7799 \pm 0.0084 (50)	0.4188 \pm 0.0123 (35)	0.8678 \pm 0.0099 (25)

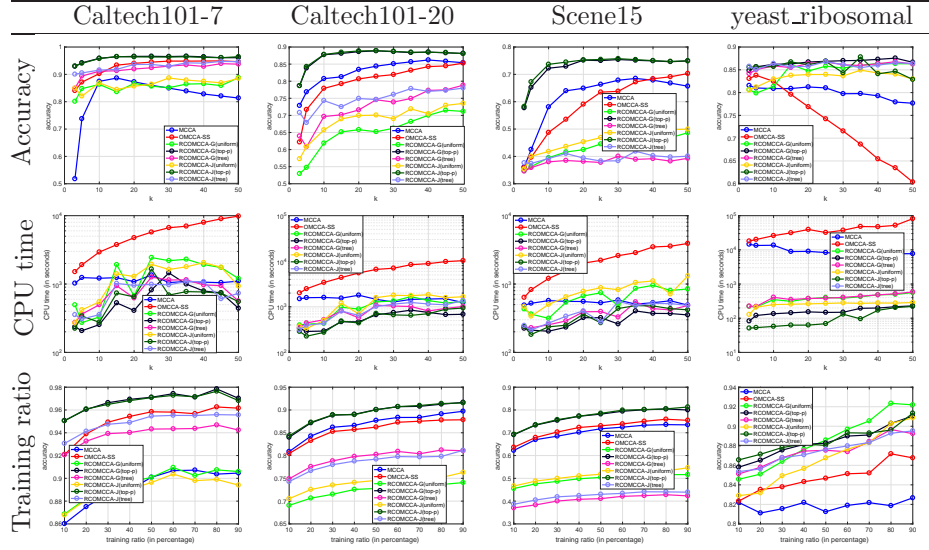


FIGURE 4. Accuracy and CPU time of three MCCA methods on four datasets by varying the reduced dimension k and the training ratio.

We use 1-nearest neighbor classifier as the base classifier for evaluating the performance of multi-view feature extraction. We run CCA methods to generate embeddings by varying $k \in \{3, 4, 5, 6\}$ for mfeat, and $k \in \{3, 5, 10, 15, 20, 25, 30, 35, 40, 45, 50\}$ for other datasets. We split the data into training and testing with the ratio 30/70. Classification accuracy is used as the performance evaluation criterion. The experimental results are reported based on the average of 10 randomly drawn splits.

We first compare eight variants of CCA methods and the classifiers based on each single view using all input features. Table 4 shows the results over five multi-view datasets with the best k shown in bracket for each method. From Table 4, we have the following observations:

- (1) CCA-based methods can achieve competitive or better results using a small set of features comparing with the best single view of the input features.
- (2) OCCA methods including RCOMCCA (top- p) and OMCCA-SS generally show better results than classical MCCA. This implies that orthogonality constraints added to MCCA can improve the learning performance.
- (3) Our proposed RCOMCCA methods with top- p weighting scheme demonstrates much better results than MCCA and OMCCA-SS can with large margins. Except for yeast_ribosomal, RCOMCCA-G (top- p) and RCOMCCA-J (top- p) outperform the classifier of the best single view on the other four datasets.
- (4) RCOMCCA with top- p weighting scheme outperforms RCOMCCA with other two scheme. This implies that pairs of views could contribute differently to the downstream classification problem.

- (5) For the same weighting schemes, our proposed RCOMCCA methods with Gauss-Seidel-style and Jacobi-style show almost similar results. It is recommended to take the problem structure into account for selecting the proper solver for efficiency as discussed in Section 5.

We also compare eight variants of CCA methods in terms of three other measurements including the sensitivity of parameter k , the CPU time, and the sampling ratio of training and testing data. The results are shown in Fig. 4. It is clear to see that

- (1) Accuracies of all CCA methods are increasing with k . However, MCCA on Caltech101-7 and OMCCA-SS on yeast_ribosomal behaves abnormally since the performance degrades significantly after a small k .
- (2) RCOMCCA generally is the most efficient method than OMCCA-SS and MCCA. Due to the incremental optimization scheme, OMCCA-SS takes linear computational complexity with k , and so its CPU time increases with k . MCCA becomes less efficient if the total number of features in all views are large, for example, on yeast_ribosomal because the analytic solution is dependent of the generalized eigenvalue problem. As shown in Fig. 4, on yeast_ribosomal, MCCA also takes more than 10 times longer than RCOMCCA.
- (3) All methods demonstrate better performance when the number of training data increases. One notable exception is MCCA on yeast_ribosomal, which does not show much gain as training data ratio increases significantly. All orthogonally constrained CCAs do not show this issue.

These observations imply that our proposed RCOMCCA not only can achieve noticeably better performance but also much faster than OMCCA-SS and MCCA for multi-view feature extraction.

7. CONCLUSION

In this paper, we start by proposing an efficient algorithm for solving CCA with orthogonality constraints, often called orthogonal CCA. Then to model the data with more than two views, we presented a novel weighted multiset CCA again with orthogonality constraints. Both algorithms rely on the solution of a subproblem with trace-fractional structure, which is solved by a newly proposed SCF iteration. Theoretically, we performed a global and local convergence analysis. Extensive experiments are conducted for evaluating the proposed algorithms against existing methods in terms of various measurements, including sensitivity analysis, correlation analysis, computation analysis, and data visualization. We further apply our methods to two real world applications: multi-label classification and multi-view feature extraction. Experimental results show that our methods not only perform competitively to or better than baselines in terms of accuracy but also are more efficient. This work focuses on the linear orthogonal projection. In the future, we would like to explore similar ideas for nonlinear CCA and other variants of CCAs with orthogonality constraints.

REFERENCES

- [1] P.-A. Absil, C. G. Baker, and K. A. Gallivan. Trust-region methods on Riemannian manifolds. *Found. Comput. Math.*, 7(3):303–330, 2007.

- [2] P.-A. Absil, R. Mahony, and R. Sepulchre. *Optimization Algorithms On Matrix Manifolds*. Princeton University Press, 2008.
- [3] Shotaro Akaho. A kernel method for canonical correlation analysis. *International Meeting on Psychometric Society*, 2001.
- [4] E. Anderson, Z. Bai, C. Bischof, J. W. Demmel, J. Dongarra, J. Du Croz, A. Greenbaum, S. Hammarling, A. McKenney, S. Ostrouchov, and D. Sorensen. *LAPACK Users' Guide*. SIAM, Philadelphia, 3rd edition, 1999.
- [5] Galen Andrew, Raman Arora, Jeff Bilmes, and Karen Livescu. Deep canonical correlation analysis. In *International conference on machine learning*, pages 1247–1255, 2013.
- [6] Z. Bai, D. Lu, and B. Vandereycken. Robust rayleigh quotient minimization and nonlinear eigenvalue problems. *SIAM J. Sci. Comput.*, 40:A3495–A3522, 2018.
- [7] Zhaojun Bai, J. Demmel, J. Dongarra, A. Ruhe, and H. van der Vorst (editors). *Templates for the solution of Algebraic Eigenvalue Problems: A Practical Guide*. SIAM, Philadelphia, 2000.
- [8] Matthew R Boutell, Jiebo Luo, Xipeng Shen, and Christopher M Brown. Learning multi-label scene classification. *Pattern recognition*, 37(9):1757–1771, 2004.
- [9] Deng Cai and Xiaofei He. Orthogonal locality preserving indexing. In *Proceedings of the 28th annual international ACM SIGIR conference on Research and development in information retrieval*, pages 3–10. ACM, 2005.
- [10] Y. Cai, L.-H. Zhang, Z. Bai, and R.-C. Li. On an eigenvector-dependent nonlinear eigenvalue problem. *SIAM J. Matrix Anal. Appl.*, 39(3):1360–1382, 2018.
- [11] D. Chu, L. Liao, M. K. Ng, and X. Zhang. Sparse kernel canonical correlation analysis. In *Proceedings of the International MultiConference of Engineers and Computer Scientists 2013*, volume I of *IMECS 2013*, Hong Kong, March 2013.
- [12] J. P. Cunningham and Z. Ghahramani. Linear dimensionality reduction: Survey, insights, and generalizations. *J. Mach. Learning Res.*, 16:2859–2900, 2015.
- [13] J. Demmel. *Applied Numerical Linear Algebra*. SIAM, Philadelphia, PA, 1997.
- [14] Paramveer Dhillon, Dean P Foster, and Lyle H Ungar. Multi-view learning of word embeddings via cca. In *Advances in neural information processing systems*, pages 199–207, 2011.
- [15] Dheeru Dua and Casey Graff. UCI machine learning repository, 2017.
- [16] G. H. Golub and C. F. Van Loan. *Matrix Computations*. Johns Hopkins University Press, Baltimore, Maryland, 4th edition, 2013.
- [17] David R Hardoon, Janaina Mourao-Miranda, Michael Brammer, and John Shawe-Taylor. Un-supervised analysis of fmri data using kernel canonical correlation. *NeuroImage*, 37(4):1250–1259, 2007.
- [18] David R Hardoon, Sandor Szedmak, and John Shawe-Taylor. Canonical correlation analysis: An overview with application to learning methods. *Neural computation*, 16(12):2639–2664, 2004.
- [19] R. A. Horn and C. R. Johnson. *Topics in Matrix Analysis*. Cambridge University Press, Cambridge, 1991.
- [20] H. Hotelling. Relations between two sets of variates. *Biometrika*, 28(3-4):321–377, 1936.
- [21] Sham M Kakade and Dean P Foster. Multi-view regression via canonical correlation analysis. In *International Conference on Computational Learning Theory*, pages 82–96. Springer, 2007.
- [22] Jon R Kettenring. Canonical analysis of several sets of variables. *Biometrika*, 58(3):433–451, 1971.
- [23] Arto Klami, Seppo Virtanen, and Samuel Kaski. Bayesian canonical correlation analysis. *Journal of Machine Learning Research*, 14(Apr):965–1003, 2013.
- [24] A. V. Knyazev. Toward the optimal preconditioned eigensolver: Locally optimal block preconditioned conjugate gradient method. *SIAM J. Sci. Comput.*, 23(2):517–541, 2001.
- [25] A. V. Knyazev and K. Neymeyr. Efficient solution of symmetric eigenvalue problems using multigrid preconditioners in the locally optimal block conjugate gradient method. *Electron. Trans. Numer. Anal.*, 15:38–55, 2003.
- [26] Effrosyni Kokiopoulou and Yousef Saad. Orthogonal neighborhood preserving projections: A projection-based dimensionality reduction technique. *IEEE Transactions on Pattern Analysis and Machine Intelligence*, 29(12):2143–2156, 2007.

- [27] Svetlana Lazebnik, Cordelia Schmid, and Jean Ponce. Beyond bags of features: Spatial pyramid matching for recognizing natural scene categories. In *2006 IEEE Computer Society Conference on Computer Vision and Pattern Recognition (CVPR'06)*, volume 2, pages 2169–2178. IEEE, 2006.
- [28] Fei-Fei Li, Rob Fergus, and Pietro Perona. Learning generative visual models from few training examples: An incremental bayesian approach tested on 101 object categories. *Computer vision and Image understanding*, 106(1):59–70, 2007.
- [29] L. Li and Z. Zhang. Semi-supervised domain adaptation by covariance matching. *IEEE Trans. Pattern Anal. Mach. Intell.*, 2019. to appear.
- [30] R. M. Martin. *Electronic Structure: Basic Theory and Practical Methods*. Cambridge University Press, Cambridge, UK, 2004.
- [31] Allan Aasbjerg Nielsen. Multiset canonical correlations analysis and multispectral, truly multitemporal remote sensing data. *IEEE transactions on image processing*, 11(3):293–305, 2002.
- [32] Jorge Nocedal and Stephen Wright. *Numerical Optimization*. Springer, 2nd edition, 2006.
- [33] Timo Ojala, Matti Pietikäinen, and Topi Mäenpää. Multiresolution gray-scale and rotation invariant texture classification with local binary patterns. *IEEE Transactions on Pattern Analysis & Machine Intelligence*, (7):971–987, 2002.
- [34] Aude Oliva and Antonio Torralba. Modeling the shape of the scene: A holistic representation of the spatial envelope. *International journal of computer vision*, 42(3):145–175, 2001.
- [35] Piyush Rai and Hal Daume. Multi-label prediction via sparse infinite cca. In *Advances in Neural Information Processing Systems*, pages 1518–1526, 2009.
- [36] Y. Saad, J. R. Chelikowsky, and S. M. Shontz. Numerical methods for electronic structure calculations of materials. *SIAM Rev.*, 52(1):3–54, 2010.
- [37] Mehmet Emre Sargin, Yücel Yemez, Engin Erzin, and A Murat Tekalp. Audiovisual synchronization and fusion using canonical correlation analysis. *IEEE Transactions on Multimedia*, 9(7):1396–1403, 2007.
- [38] Xiao-Bo Shen, Quan-Sen Sun, and Yun-Hao Yuan. Orthogonal canonical correlation analysis and its application in feature fusion. In *Proceedings of the 16th International Conference on Information Fusion*, pages 151–157. IEEE, 2013.
- [39] Xiaobo Shen and Quansen Sun. Orthogonal multiset canonical correlation analysis based on fractional-order and its application in multiple feature extraction and recognition. *Neural Processing Letters*, 42(2):301–316, 2015.
- [40] Ji-Guang Sun. *Matrix Perturbation Analysis*. Academic Press, Beijing, 1987. In Chinese.
- [41] Liang Sun, Shuiwang Ji, and Jieping Ye. Canonical correlation analysis for multilabel classification: A least-squares formulation, extensions, and analysis. *IEEE Transactions on Pattern Analysis and Machine Intelligence*, 33(1):194–200, 2010.
- [42] Grigorios Tsoumakos and Ioannis Katakis. Multi-label classification: An overview. *International Journal of Data Warehousing and Mining (IJDWM)*, 3(3):1–13, 2007.
- [43] Viivi Uurtio, João M Monteiro, Jaz Kandola, John Shawe-Taylor, Delmiro Fernandez-Reyes, and Juho Rousu. A tutorial on canonical correlation methods. *ACM Computing Surveys (CSUR)*, 50(6):95, 2018.
- [44] Z. Wang, Q. Ruan, and G. An. Projection-optimal local Fisher discriminant analysis for feature extraction. *Neural Comput & Applic*, 26:589–601, 2015.
- [45] Daniela M Witten, Robert Tibshirani, and Trevor Hastie. A penalized matrix decomposition, with applications to sparse principal components and canonical correlation analysis. *Biostatistics*, 10(3):515–534, 2009.
- [46] Jianixn Wu and James M Rehg. Where am i: Place instance and category recognition using spatial pact. In *2008 Ieee Conference on Computer Vision and Pattern Recognition*, pages 1–8. IEEE, 2008.
- [47] W. H. Yang, L.-H. Zhang, and R. Y. Song. Optimality conditions of the nonlinear programming on Riemannian manifolds. *Pacific J. Optim.*, 10:415–434, 2014.
- [48] Jieping Ye. Characterization of a family of algorithms for generalized discriminant analysis on undersampled problems. *Journal of Machine Learning Research*, 6(Apr):483–502, 2005.
- [49] Bo Zhang, Jie Hao, Gang Ma, Jinpeng Yue, and Zhongzhi Shi. Semi-paired probabilistic canonical correlation analysis. In *International Conference on Intelligent Information Processing*, pages 1–10. Springer, 2014.
- [50] L.-H. Zhang. Uncorrelated trace ratio LDA for undersampled problems. *Patt. Recog. Lett.*, 32:476–484, 2011.

- [51] L.-H. Zhang, L.-Z. Liao, and M. K. Ng. Fast algorithms for the generalized Foley-Sammon discriminant analysis. *SIAM J. Matrix Anal. Appl.*, 31(4):1584–1605, 2010.
- [52] Lei-Hong Zhang and Ren-Cang Li. Maximization of the sum of the trace ratio on the Stiefel manifold, I: Theory. *SCIENCE CHINA Math.*, 57(12):2495–2508, 2014.
- [53] Lei-Hong Zhang and Ren-Cang Li. Maximization of the sum of the trace ratio on the Stiefel manifold, II: Computation. *SCIENCE CHINA Math.*, 58(7):1549–1566, 2015.
- [54] Min-Ling Zhang and Zhi-Hua Zhou. Ml-knn: A lazy learning approach to multi-label learning. *Pattern recognition*, 40(7):2038–2048, 2007.
- [55] Yi Zhang and Jeff Schneider. Multi-label output codes using canonical correlation analysis. In *Proceedings of the fourteenth international conference on artificial intelligence and statistics*, pages 873–882, 2011.